

AN INTERSTELLAR ORIGIN FOR THE BERYLLIUM 10 IN CALCIUM-RICH, ALUMINUM-RICH INCLUSIONS

S. J. DESCH¹

Department of Terrestrial Magnetism, Carnegie Institution of Washington, 5241 Broad Branch Road W, Washington, DC 20015;
and NASA Astrobiology Institute; desch@dtm.ciw.edu

HAROLD C. CONNOLLY, JR.

Kingsborough College, City University of New York, CUNY, Department of Physical Sciences, 2001 Oriental Boulevard, Brooklyn, NY 11235; and
American Museum of Natural History, Department of Earth and Planetary Sciences, Central Park West at 79th Street, New York, NY 10024;
and Rutgers University, Department of Geological Sciences, 610 Taylor Road, Piscataway, NJ 08854; hconnolly@kbcc.cuny.edu

AND

G. SRINIVASAN²

Physical Research Laboratory, Ahmedabad 380 009, India; srini@prl.ernet.in

Received 2003 March 27; accepted 2003 October 15

ABSTRACT

Beryllium 10 is a short-lived radionuclide ($t_{1/2} = 1.5$ Myr) that was incorporated live into calcium-rich, aluminum-rich inclusions (CAIs) at the birth of our solar system. Beryllium 10 is unique among the short-lived radionuclides in that it is formed only by spallation reactions and not by nucleosynthesis, e.g., in a supernova. Recent work by McKeegan, Gounelle, and others has stated that the high initial abundance of ^{10}Be in CAIs ($^{10}\text{Be}/^9\text{Be} \approx 1 \times 10^{-3}$) cannot be attributed to galactic cosmic rays (GCRs) and therefore concluded that the spallation reactions must have occurred within the solar nebula itself, because of energetic particles emitted by the early Sun. In this paper we reexamine this conclusion. We calculate the contributions of GCRs to the ^{10}Be abundance in a molecular cloud core as it collapses to form a protostar and protoplanetary disk. We constrain the flux of protons and ^{10}Be GCRs in the Sun's molecular cloud core 4.5 Gyr ago. We use numerical magneto-hydrodynamic simulations of star formation to model the time evolution of the magnetic field strength and column density of gas in a collapsing cloud core. We account for magnetic focusing and magnetic mirroring and the anisotropic distribution of GCR pitch angles in the cloud core. We calculate the rates at which GCR protons and α -particles induce spallation reactions producing ^{10}Be atoms, and the rates at which GCR ^{10}Be nuclei are trapped in the cloud core. Accounting also for the decay of ^{10}Be over the evolution of the cloud core, we calculate the time-varying $^{10}\text{Be}/^9\text{Be}$ ratio. We find that at the time of protostar formation $^{10}\text{Be}/^9\text{Be} \approx 1 \times 10^{-3}$, with an uncertainty of about a factor of 3. Spallation reactions account for 20% of the ^{10}Be in CAIs, while trapped GCR ^{10}Be nuclei account for the other 80%. The initial abundance of ^{10}Be in CAIs is therefore entirely attributable to cosmic rays. We discuss the implications of this finding for the origin of other short-lived radionuclides and for the use of ^{10}Be as a chronometer.

Subject headings: cosmic rays — nuclear reactions, nucleosynthesis, abundances — solar system: formation — stars: formation

1. BACKGROUND

Beryllium 10 (^{10}Be) is a short-lived radionuclide whose one-time presence in calcium-rich, aluminum-rich inclusions (CAIs) in chondrites was discovered only 3 years ago (McKeegan, Chaussidon, & Robert 2000a, 2000b). The evidence for live radioactive ^{10}Be at the birth of the solar system has been recognized for its potential to constrain the production mechanism of the other radionuclides in meteorites and the mode of formation of our solar system itself. In fact, the existence of ^{10}Be has been labeled potentially the “smoking gun” that proves that the short-lived radionuclides in CAIs formed by particle irradiation in the solar nebula (Gounelle et al. 2001). If true, the case for a supernova triggering the formation of the solar system and injecting it with radio-

nuclides (Cameron & Truran 1977) is greatly weakened. The fundamental question of how our molecular cloud collapsed to form our solar system even today remains unanswered. The newly found evidence for ^{10}Be in CAIs is the key to unlocking the riddle of our solar system's origin.

Evidence for the one-time presence of ^{10}Be in CAIs comes from excesses of ^{10}B that correlate with their beryllium abundance. Beryllium 10 decays to ^{10}B with a mean life of 2.18 Myr (Firestone et al. 1996). Within several minerals in individual CAIs the abundances of ^9Be , ^{10}B , and ^{11}B are measured; if the ratio $^{10}\text{B}/^{11}\text{B}$ is linearly correlated with the $^9\text{Be}/^{11}\text{B}$ ratio, the excess ^{10}B can be attributed to the decay of ^{10}Be . The slope of the correlation gives the $^{10}\text{Be}/^9\text{Be}$ ratio at the time of isotopic closure (last crystallization). Table 1 lists all $^{10}\text{Be}/^9\text{Be}$ ratios inferred to date in 16 CAIs (McKeegan et al. 2000a, 2000b; Chaussidon et al. 2001; MacPherson & Huss 2001; Sugiura, Shuzou, & Ulyanov 2001; Srinivasan 2002). The inferred $^{10}\text{Be}/^9\text{Be}$ ratios in these analyses all lie in the range $(4.5\text{--}18) \times 10^{-4}$. Further refinements in these ratios may be possible; for example, if the initial $^{11}\text{B}/^{10}\text{B}$ ratio of the CAIs is taken to be fixed at the chondritic value instead of as a

¹ Current address: Department of Physics and Astronomy, Arizona State University, P.O. Box 871504, Tempe, AZ 85287; steve.desch@asu.edu.

² Current address: Department of Geology, Earth Sciences Centre, University of Toronto, 22 Russell Street, Toronto, ON M5S 3B1, Canada; srini@geology.utoronto.ca.

TABLE 1
 $^{10}\text{Be}/^9\text{Be}$ RATIOS MEASURED IN CAIS

CAI	Type	$(^{10}\text{Be}/^9\text{Be})/10^{-4}$	Reference
Allende 001.....	B	5.3 ± 0.24	1
Allende 002.....	B	6.7 ± 0.10	1
Allende 3529-Z.....	B	7.6 ± 2.6	2
Allende 3529-41.....	B	9.5 ± 1.9	3
Efremovka E54.....	B	4.5 ± 1.3	2
Efremovka E38.....	B	6.0 ± 1.2	1
Efremovka E69.....	B	6.1 ± 1.9	1
Efremovka E107.....	B	6.5 ± 2.4	2
Efremovka E44.....	B	7.6 ± 1.9	1
Efremovka E44.....	B	8.3 ± 2.2	2
Efremovka E48.....	A/B	8.1 ± 3.1	2
Efremovka E65.....	B	18.2 ± 4.6	4
Vigarano 477-4b.....	B	7.8 ± 8.8	5
Vigarano 1623-9.....	A	11 ± 5	5
Vigarano 477-5.....	A	16 ± 8	5
Leoville 3535-3b.....	A	8 ± 1.2	5
Axtell 2771.....	FUN	4.6 ± 3.2	5

REFERENCES.—(1) Sugiura et al. 2001; (2) Chaussidon et al. 2001; (3) McKeegan et al. 2000b; (4) Srinivasan 2002; (5) MacPherson & Huss 2001.

free parameter, the variations in the $^{10}\text{Be}/^9\text{Be}$ ratio are tightened. MacPherson & Huss (2001) in their analysis found that the spread went from a factor of 3.5 to only 2.5, simultaneously reducing the error estimates on some marginal detections (e.g., Vigarano 477-4b). At any rate, the data as they stand are consistent with the canonical initial ratio inferred by McKeegan et al. (2000b), $\approx 9.5 \times 10^{-4}$, which we adopt. Of the 16 CAIs, only in Efremovka E65 does the initial $^{10}\text{Be}/^9\text{Be}$ ratio exceed the canonical value by a statistically significant amount. More important, in every CAI that has been searched, evidence for ^{10}Be has been found; in no CAI has ^{10}Be been demonstrated to have been absent. Augmenting these data are inferred initial $^{10}\text{Be}/^9\text{Be}$ ratios from hibonite residues in Murchison and Allende: $\sim 8 \times 10^{-4}$ (Murchison CH-B7) and $\sim 4 \times 10^{-4}$ (Murchison SH-7), from Marhas, Goswami, & Davis (2002); and $\approx 8.0 \times 10^{-4}$ (Murchison CH-C4) and $\approx 4.4 \times 10^{-4}$ (Allende HAL), from Marhas & Goswami (2003). (We have not included Murchison CH-C1 since its initial ratio is based on only two analyses.) These data are again consistent with the canonical initial ratio $\approx 9.5 \times 10^{-4}$ and suggest that ^{10}Be was uniformly widespread in the solar nebula.

Radionuclides such as ^{10}Be can be used to constrain the mode of our solar system's formation. For example, the presence of ^{26}Al (mean life 1.03 Myr) and ^{41}Ca (mean life 0.15 Myr) in meteorites may be attributable to a supernova that injected these radionuclides as it triggered the collapse of our solar system's molecular cloud (see review by Goswami & Vanhala 2000). Unlike ^{26}Al and ^{41}Ca and unique among the short-lived radionuclides, ^{10}Be must be formed by spallation, either involving galactic cosmic rays (GCRs) or by energetic particles in the solar nebula (although production in a supernova jet has been speculated on; Cameron 2001). If GCR spallation can be ruled out, then irradiation within the solar nebula is required to explain the presence of ^{10}Be , which would then indeed be the "smoking gun" for in situ particle irradiation. One in situ irradiation model is the "X-wind" model (Shu, Shang, & Lee 1996, 1997, 2001; Lee et al. 1998; Gounelle et al. 2001). In these papers it is claimed that the

short-lived radionuclides such as ^{26}Al and ^{41}Ca , as well as ^{10}Be , can be coproduced in the proportions found in CAIs. If true, then contributions to ^{26}Al and ^{41}Ca from external sources such as a nearby supernova effectively would be ruled out. This would remove the prime motivation for models in which the collapse of the solar system's molecular cloud was triggered by a supernova.

Young stars are copious producers of X-rays by magnetic flares and presumably also the MeV particles capable of producing ^{10}Be by spallation. The challenge in producing radionuclides by irradiation from the proto-Sun is that material must be irradiated much closer to the proto-Sun (~ 0.1 AU) than 3 AU to match the meteoritic radionuclide abundances (Goswami, Marhas, & Sahijpal 2001). Transport of material from the early Sun to the 2–3 AU region whence the meteorites originate is then problematic. The X-wind model (Shu et al. 2001; Gounelle et al. 2001) seeks to resolve the irradiation and transport issues within the framework of a single astrophysical model, hypothesizing that CAIs are thermally processed and irradiated by energetic particles at 0.1 AU and then are launched in a disk wind to the asteroid belt region. The combination of these physical effects is the essence of the X-wind model. There are caveats associated with the X-wind model. It is not clear that CAIs would be thermally processed near the proto-Sun in ways consistent with their petrology and chemical abundances (see § 7). There are also caveats associated with the irradiation mechanism itself. The first is that the spectrum of energetic particles assumed in the X-wind model is much more effective at producing ^{10}Be than the other short-lived radionuclides. For most parameters in the Gounelle et al. (2001) model, if the $^{10}\text{Be}/^9\text{Be}$ is produced at its canonical ratio, then the other ratios (e.g., $^{26}\text{Al}/^{27}\text{Al}$) are below canonical. Only under optimal conditions (e.g., high ^3He flux) did Gounelle et al. (2001) coproduce the radionuclides ^{26}Al , ^{41}Ca , and ^{53}Mn with ^{10}Be (see § 7). The second caveat is that production of ^{10}Be should not be attributed to in situ irradiation unless external sources of ^{10}Be have been ruled out. If some fraction of ^{10}Be is attributable to contributions from GCRs, then the flux of energetic particles producing the ^{10}Be would have to be scaled back accordingly. In the X-wind model, this would mean that other radionuclides would be produced at levels well below their canonical ratios. If *all* the ^{10}Be in CAIs could be attributed to GCRs, then *none* of the other short-lived radionuclides could be explained by the X-wind model. More generally, because particle irradiation from young stars produces ^{10}Be so effectively (relative to other radionuclides), in situ irradiation models (such as the X-wind) can effectively be ruled out if an external source of ^{10}Be is identified.

Low values of the $^{10}\text{Be}/^9\text{Be}$ ratio, more than an order of magnitude below canonical, have been predicted under the assumption that GCRs are the only source of ^{10}Be . The two papers that make this prediction, McKeegan et al. (2000b) and Gounelle et al. (2001), use this prediction to rule out an external cosmic-ray origin for ^{10}Be . This conclusion is premature in that both analyses consider only the rate at which GCR protons and α -particles can induce spallation reactions that produce ^{10}Be , and they do not consider contributions from GCRs that are themselves ^{10}Be nuclei. Moreover, repeating the analyses of Gounelle et al. (2001) and McKeegan et al. (2000b), we find that even in the context of direct reactions alone the discrepancies between the theoretical predictions and the canonical ratio are *less* than an order of magnitude. For example, Gounelle et al. (2001) consider the steady state $^{10}\text{Be}/^9\text{Be}$ ratio as a function of Galactic history in a simplified

evolution model. They calculate the production of both ^{10}Be and ^9Be over the lifetime of the Galaxy due to spallation reactions between GCR protons and α -particles and interstellar CNO nuclei, including the effects of astration. The abundance of ^9Be rises steadily over the ≈ 8 Gyr of Galactic evolution before the Sun's birth, but the abundance of ^{10}Be is sensitive only to the previous few Myr of evolution, because of its short half-life. The short-lived radionuclide ^{10}Be is continually diluted by the stable isotope ^9Be . Gounelle et al. (2001) claim that matching the meteoritic ratio $^{10}\text{Be}/^9\text{Be} \sim 10^{-3}$ would require an increase in the GCR flux for the few Myr prior to the solar system's birth, relative to the previous 8 Gyr, of a factor of 20 (as implied in their § 4). However, in their best-case scenario (the doubly thick case of their Appendix B in which ^{10}Be is easily retained), the stated discrepancy is only $8\mathcal{A}_s^{-1}$, and $\mathcal{A}_s = 0.87$, yielding a discrepancy of 9.1, not 20. We repeat their same calculation and find an even smaller discrepancy. The appropriate factor by which the GCR flux must increase to match the meteoritic ratio (for their "doubly thick" case) is actually $(9 \times 10^{-4}) / (^{10}\text{Be}/^9\text{Be})_{\text{pred}} = (9 \times 10^{-4}) / (1.1 \times 10^{-4} \mathcal{A}_s^{-1}) = 8\mathcal{A}_s^{-1}$ (not $8\mathcal{A}_s^{-1}$). Also, using their definition of the astration factor $\mathcal{A}_s \equiv (\tau_*/t)[1 - \exp(-t/\tau_*)]$, with $\exp(-15 \text{ Gyr}/\tau_*) = 0.50$, and $t = 10$ Gyr, we find $\mathcal{A}_s = 0.80$ (not 0.87). Therefore, the actual discrepancy is only 6.6, less than 20 by a factor of 3. Some increase in GCR flux (relative to the average of the previous 8 Gyr) is required to match the canonical $^{10}\text{Be}/^9\text{Be}$ ratio by spallation reactions, but it is less than an order of magnitude.

Low levels of the $^{10}\text{Be}/^9\text{Be}$ ratio were also predicted by McKeegan et al. (2000b) by using a different model. They recognized that the solar abundance of beryllium, $^9\text{Be}/\text{H} = 2.6 \times 10^{-11}$ (Anders & Grevesse 1989), is a fixed and known quantity, so the $^{10}\text{Be}/^9\text{Be}$ ratio depends only on the abundance of ^{10}Be , which is sensitive only to the previous few Myr of Galactic history. Using a GCR production rate of ^9Be per H atom of 10^{-21} yr^{-1} (Prantzos, Vangioni-Flam, & Casse 1993b) and the production branching ratio $^{10}\text{Be}/^9\text{Be} = 0.1$, McKeegan et al. (2000b) estimated the steady state abundance $^{10}\text{Be}/^9\text{Be} \approx 8 \times 10^{-6}$, about 2 orders of magnitude short of the meteoritic ratio. We note, though, that Lemoine, Vangioni-Flam, & Casse (1998) estimate a present-day production rate of ^9Be of $\approx 6 \times 10^{-21} \text{ yr}^{-1} \text{ H}^{-1}$, which yields a steady state ratio 5×10^{-5} . Since the GCR flux was a factor of 2 higher 4.5 Gyr ago than today (§ 4.2), a solar system ratio $^{10}\text{Be}/^9\text{Be} \sim 10^{-4}$ from direct spallation reactions is likely. To explain the meteoritic $^{10}\text{Be}/^9\text{Be}$ ratio by spallation reactions would require an increase in the GCR flux by a factor of less than 10 (relative to the expected average in the Galaxy 4.5 Gyr ago). We accept the conclusion that spallation reactions are incapable of producing the observed ^{10}Be in CAIs but note that the discrepancies are $\lesssim 10$, not $\sim 10^2$, for the McKeegan et al. (2000b) model, and only ≈ 6 , not ~ 20 , for the Gounelle et al. (2001) model.

Inspired by the much reduced discrepancies, we are motivated to consider other contributions to ^{10}Be from GCRs. One contribution that has never been quantified is the trapping of cosmic rays in a molecular cloud core as it collapses. This mechanism was suggested by Clayton & Jin (1995) as one possible source of ^{26}Al in the early solar system. They recognized the coincidence in the stopping lengths of low-energy (~ 10 MeV nucleon $^{-1}$) cosmic rays and the column densities of molecular cloud cores, $\approx 0.01 \text{ g cm}^{-2}$ (van Dishoeck et al. 1993). By our own estimates, this mechanism fails to explain the meteoritic $^{26}\text{Al}/^{27}\text{Al}$ ratio (§ 7). Clayton also suggested the

same mechanism as the source of ^{10}Be in the early solar system (quoted in Gounelle et al. 2001). Given the high abundance of ^{10}Be nuclei in GCRs (Be is present at levels 10^6 times solar!), we consider it possible that GCR ^{10}Be nuclei trapped in a molecular cloud could contribute significantly to the $^{10}\text{Be}/^9\text{Be}$ ratio.

Using the numerical simulations of Desch & Mouschovias (2001, hereafter DM01) as a model for the evolution of a molecular cloud core's magnetic field strength and column density of gas, we perform the first numerical calculations of the GCR contributions to a short-lived radionuclide in a molecular cloud core. These numerical simulations are discussed in § 2. In § 3 we discuss the ability of GCRs to penetrate into such molecular cloud cores. In § 4 we constrain the GCR flux of H and He nuclei over the energy range relevant for direct spallation reactions, and the flux of ^{10}Be GCRs at low energies. We then extrapolate these fluxes to conditions in the Sun's molecular cloud core 4.5 Gyr ago. In § 5 we present formulas for the contributions of GCRs to the solar system's ^{10}Be inventory, by direct reactions and by trapping of GCRs in the cloud core. We present results in § 6, including the time evolution of the $^{10}\text{Be}/^9\text{Be}$ ratio, and the dependence of $^{10}\text{Be}/^9\text{Be}$ on the starting magnetic field strength of the cloud core. On the basis of our calculations we would predict a ratio $^{10}\text{Be}/^9\text{Be} \approx 1 \times 10^{-3}$ in the early solar nebula, with uncertainties on the order of a factor of 3. This ratio is completely consistent with the level found in CAIs. In § 7 we discuss the many implications of this result in regard to meteoritics and the formation of the solar system.

2. COLLAPSE OF MOLECULAR CLOUD CORES

Molecular cloud cores, dense condensations within molecular clouds, are the sites of star formation. Molecular clouds have typical densities $\sim 10^3 \text{ cm}^{-3}$, temperatures ~ 10 K, and span several parsecs or more. They are threaded by magnetic fields of order $\sim 5 \mu\text{G}$ (Crutcher 1999). Within them, a multitude of molecular cloud cores may form, although the process by which clouds fragment into cores is not well understood. Molecular cloud cores are denser, $\sim 10^4 \text{ cm}^{-3}$, span only ~ 0.1 pc, and contain $\sim 1 M_\odot$ of molecular gas. Their magnetic field strengths are determined by OH Zeeman measurements to be comparable to 10–15 μG (Crutcher 1999). Their column densities are typically greater than several visual extinctions, or several times $10^{-2} \text{ g cm}^{-2}$. As each cloud core collapses, one or more stars are formed within it. This process is observationally constrained to take several Myr from the time that an identifiable core forms until a star forms in it (e.g., van Dishoeck et al. 1993; Ward-Thompson 2002).

To model the entry and trapping of cosmic rays in a molecular cloud core, we must specify the evolution of the magnetic field and the column density of gas. The column density and magnetic field strength in a collapsing cloud core evolve on the same Myr timescales on which ^{10}Be decays. Cosmic rays lose kinetic energy in ionizing the gas molecules, which slows them and allows them to be trapped. Generally, the magnetic field in a molecular cloud core may possess two components, one ordered and one disordered, tangled by turbulent motions. On average, the ordered component of field lines are focused into cloud cores; GCRs, being charged, follow the field lines and are focused into the core. The converging field lines also increase the pitch angles of GCRs and can mirror the cosmic rays out of the cloud core. The turbulent disordered field also has local regions of enhanced magnetic field strength that can scatter GCRs in pitch angle. On scales

larger than the scales on which turbulence affects the magnetic field strength, scattering would tend to enhance trapping and spallation by increasing the amount of gas the GCRs interact with. Magnetohydrodynamic turbulence is unable to distort the magnetic field on small scales ~ 0.1 pc because ion-neutral collisions are predicted to damp the turbulence (Kulsrud & Pearce 1969; Mouschovias 1991). The supersonic velocity dispersions associated with turbulence are observed not to act on scales less than 0.1 pc (Ossenkopf & Mac Low 2002). We neglect the effects of turbulence on the propagation of GCRs into cloud cores.

Even as the magnetic field affects the propagation of GCRs, it plays a critical role in the evolution of molecular cloud cores. Regardless of the external pressure, cloud cores cannot collapse so long as the mass-to-flux ratio of column density Σ to (ordered) magnetic field strength B is below a critical value $(\Sigma/B)_{\text{crit}} = 0.126 G^{-1/2}$ (Mouschovias & Spitzer 1976; Tomisaka, Ikeuchi, & Nakamura 1988). Because of its importance, the mass-to-flux ratio is often normalized to this critical value in the parameter $\mu_{c0} = (\Sigma/B)/(\Sigma/B)_{\text{crit}}$, so a necessary condition for collapse is $\mu_{c0} > 1$. The physical reason for this condition is that to a good approximation magnetic field lines are frozen in the gas, so that gravitational contraction leads to an increase in expansive magnetic energy. Cloud cores with $\mu_{c0} < 1$ do not contract and are termed magnetically subcritical, while in cloud cores with $\mu_{c0} > 1$ the magnetic field cannot prevent the collapse, and such cloud cores are magnetically supercritical.

No observations to date have definitively settled the issue of whether molecular cloud cores are magnetically subcritical or supercritical (i.e., what is μ_{c0} in cloud cores?). Zeeman measurements can yield only the line-of-sight component of the ordered magnetic field B , and if the field lines are inclined by an angle θ to the line of sight, the inferred B will underestimate the actual field strength by a factor of $\cos \theta$. In addition, if cloud cores are flattened along the magnetic field direction (see below), the measured column densities will overestimate the true column density of the cloud core by a factor of $1/\cos \theta$. One expects that the μ_{c0} inferred for cloud cores may overestimate the true mass-to-flux ratios by a factor of $1/\cos^2 \theta$, which is ≈ 3 on average. Crutcher (1999) has found for a sample of 27 cloud cores that $\mu_{c0} = 1.7 \pm 0.2$ if they are not flattened along the magnetic field and $\mu_{c0} = 1.1 \pm 0.2$ if they are. Assuming flattening along field lines, the data of Crutcher (1999) have been shown to be consistent with $0.5 \lesssim \mu_{c0} \lesssim 1.5$ (Ciolek & Basu 2001; Shu et al. 1999; Table 1). Molecular cloud cores appear to be very near a critical state in which the magnetic field must play a major role in the dynamics and may even be able to support the cloud core against collapse.

Sharp distinctions are often made in the literature between those cloud cores with $\mu_{c0} < 1$, which are characterized as being supported against collapse by the magnetic field, evolving slowly only because of ambipolar diffusion, and those with $\mu_{c0} > 1$, which are characterized as being in rapid, nearly free-fall collapse (e.g., Bourke et al. 2001). In fact, cloud cores with $\mu_{c0} < 1$ and $\mu_{c0} > 1$ probably tend to form a continuous spectrum of states. In cloud cores with $\mu_{c0} > 1$, the magnetic field does not entirely prevent collapse, but it greatly slows down the collapse by diluting the gravitational acceleration. Collapse proceeds on timescales greater than the standard free-fall timescale $\tau_{\text{ff}} = (3\pi/32G\rho)^{-1/2}$, where ρ is the density of the cloud core. In numerical simulations of the inner regions of collapsing molecular cloud cores, with

$\mu_{c0} \approx 1.5-2$, collapse is slowed to timescales $\sim 2\tau_{\text{ff}}$ (Fiedler & Mouschovias 1993; DM01). In cloud cores with $\mu_{c0} < 1$, magnetic forces can support the cloud core indefinitely, assuming ideal coupling between the ions and electrons (on which the magnetic forces act) and the neutrals (making up the majority of the gas). In reality, because the abundance of electrons and ions relative to neutrals is $\lesssim 10^{-7}$ (Williams et al. 1998), neutral molecules can gravitationally settle in the core center by diffusing through the ions and electrons, which remain fixed to the stationary field lines. The characteristic timescale for this process is the ambipolar diffusion timescale $\tau_{\Phi} \sim \tau_{\text{ff}}^2/\tau_{\text{ni}} \sim 10\tau_{\text{ff}}$ in typical cloud cores, where τ_{ni} is the timescale for momentum exchange between ions and neutrals (Mouschovias 1991). The actual collapse timescale of a cloud core with $\mu_{c0} < 1$ is a factor of order unity times this characteristic timescale. Ciolek & Basu (2001) have shown that for $0.5 < \mu_{c0} < 0.8$, the actual collapse timescale is $(1 - \mu_{c0})\tau_{\Phi}$, or roughly 2–5 free-fall timescales. We accordingly assume that the collapse timescale is $(1 - \mu_{c0})\tau_{\Phi}$ or $2\tau_{\text{ff}}$, whichever is greater.

The evolution of molecular cloud cores is modeled using the numerical simulations of DM01. The simulations of DM01 were conducted using a version of the Zeus-2D code of the Laboratory for Computational Astrophysics at the University of Illinois³ (Stone & Norman 1992a, 1992b), modified to include ambipolar diffusion, ohmic dissipation, gravitational potential in cylindrical coordinates, and detailed charge chemistry in the cloud core. They begin with a cylindrical region 0.75 pc in radius and 0.75 pc in half-thickness, filled with gas at isothermal temperature 10 K and uniform density $n_{\text{H}_2} = 300 \text{ cm}^{-3}$, which is characteristic of the molecular cloud stage. The computational volume contains $45 M_{\odot}$, and the column density through the region (along the symmetry axis) is 0.005 g cm^{-2} , which is less than the typical column density through cloud cores. DM01 neglect the effects of magnetic turbulence on the evolution of the cloud core, but it is not expected to act strongly on scales less than 0.1 pc at any rate (Mouschovias 1991; Ossenkopf & Mac Low 2002). Their simulations assume only a uniform 30 μG ordered magnetic field parallel to the symmetry axis, which yields $\mu_{c0} = 0.37$. In their simulations, DM01 found that the gas immediately collapsed on a timescale $\tau_{\text{ff}} \sim 1$ Myr along field lines to form a flattened structure characterized by column density $\Sigma_{\perp} \approx 0.01 \text{ g cm}^{-2}$ and a central density of several times 10^3 cm^{-3} . Strong observational evidence exists for cloud cores being flattened in one direction (Basu 2000), and in many cases the flattening is demonstrably along the magnetic field lines (Tamura, Hough, & Hayashi 1995). After this initial flattening, the cloud core evolves on slower timescales. In determining the contributions to ^{10}Be over the evolution of the molecular cloud core, it is essential that we begin with initial conditions such as these that predate the formation of the cloud core. We accordingly adopt this initial state (volume filled with uniform-density gas with $n_{\text{H}_2} = 300 \text{ cm}^{-3}$) for all the cases we consider below.

Having reached this initial state, the evolution of $\Sigma_{\perp}(t)$ and $B(t)$ in the molecular cloud core will depend on the initial magnetic field strength B_0 . If $B_0 < 11 \mu\text{G}$ and $\mu_{c0} > 1$, the cloud core immediately begins nearly free-fall collapse on a timescale $\sim 2\tau_{\text{ff}}$. As numerical simulations have shown (e.g., Fiedler & Mouschovias 1993; DM01), the magnetic field lines effectively remain frozen in the gas, the mass-to-flux ratio

³ See <http://zeus.nca.uiuc.edu>.

stays roughly constant, and B and Σ_{\perp} vary in direct proportion to each other. On the other hand, if $\mu_{c0} < 1$, collapse requires first that ambipolar diffusion increase the column density at the core's center, while keeping B constant, before nearly free-fall collapse can begin. This process takes a time $(1 - \mu_{c0})\tau_{\Phi}$, during which the mass-to-flux ratio μ_c steadily increases from its initial value μ_{c0} . Only when μ_c has risen above unity, at a time designated $t = t_{\text{sup}}$, can the cloud core collapse. Once $\mu_c > 1$, however, collapse proceeds exactly as it does for cloud cores with initial $\mu_{c0} > 1$, and the cloud core essentially loses memory of its initial state (Ciolek & Mouschovias references). While the numerical simulations of DM01 were conducted for one initial value of $B_0 = 30 \mu\text{G}$, they can be extrapolated to other cases by using the above theoretical results. The following relations satisfy all the above criteria and allow a reasonable approximation to the timescales, column densities Σ_{\perp} , and magnetic field strengths $B(t)$ as functions of time in cloud cores with different B_0 . In cloud cores with $\mu_{c0} < 1$, while $t \leq t_{\text{sup}}$, the cloud core is magnetically subcritical and ambipolar diffusion is operating.

$$\begin{aligned} B(t') &= B_{\text{DM01}}(t)(B_0/30 \mu\text{G}) \\ \Sigma_{\perp}(t') &= \Sigma_{\perp, \text{DM01}}(t)[1 + (t/t_{\text{sup}})(B_0/30 \mu\text{G} - 1)] \\ t'_{\text{sup}} - t' &= (t_{\text{sup}} - t)_{\text{DM01}} 1.58[1 - 0.37(30 \mu\text{G}/B_0)] \end{aligned} \quad (1)$$

After the supercritical core has formed and $t \geq t_{\text{sup}}$,

$$\begin{aligned} B(t') &= B_{\text{DM01}}(t)(B_0/30 \mu\text{G}), \\ \Sigma_{\perp}(t') &= \Sigma_{\perp, \text{DM01}}(t)(B_0/30 \mu\text{G}), \\ t' - t'_{\text{sup}} &= (t - t_{\text{sup}})_{\text{DM01}}. \end{aligned} \quad (2)$$

For initially supercritical cloud cores with $\mu_{c0} > 1$, only the relations for $t \geq t_{\text{sup}}$ are used.

Exactly what conditions are necessary to lead to the formation of a molecular cloud core in the first place are not well constrained, but we wish to emphasize that many of the uncertainties associated with star formation are irrelevant to the evolution of a cloud core once it does form. The DM01 simulations are probably robustly applicable to the problem of cosmic-ray trapping. For example, it is irrelevant whether cloud cores form in filamentary structures along magnetic field lines; cosmic rays will be stopped in one cloud core (and so not reach a second cloud core) only during the brief ($\ll 1$ Myr) stage during which the stopping cloud core is in nearly free-fall collapse. The issue of turbulence is somewhat moot because it is not expected to provide support on scales less than 0.1 pc. Magnetic turbulence would in any case prolong the early stages of collapse, as well as enhance trapping and spallation, both effects increasing the $^{10}\text{Be}/^9\text{Be}$ ratio. Uncertainties in the initial mass-to-flux ratio in the observationally determined range $0.5 \lesssim \mu_{c0} \lesssim 1.5$ are accounted for in our extrapolations. If the collapse of cloud cores is triggered by an increase in external pressure (e.g., the passage of a supernova shock in a cluster star-forming environment), it is still necessary for the cloud core to become magnetically supercritical to collapse (Mouschovias & Spitzer 1976). Finally, UV ionization is more effective in cluster environments, which (counterintuitively) reduces the ambipolar diffusion timescale τ_{Φ} but typically by no more than 30% (Ciolek & Mouschovias 1995). Independent of the star-forming environment, cloud cores must necessarily reach $\mu_{c0} > 1$ to evolve into solar systems. In doing so, observations and theory suggest collapsing cloud cores should have $\mu_{c0} < 1.5$ and should evolve

exactly as the core of DM01 did as soon as it became magnetically supercritical, with the same relationship between B and Σ_{\perp} . We expect that the collapse timescales of actual cloud cores will be matched by these model results to within a few tens of percent, on the basis of the variations seen among different numerical simulations. Likewise, the proportionality between Σ_{\perp} and B at any time is well constrained by the fact that in various numerical simulations the mass-to-flux ratio of a collapsing supercritical core is $\mu_c \approx 1.5$ to within a few tens of percent. These uncertainties translate into uncertainties in the final $^{10}\text{Be}/^9\text{Be}$ ratio of no more than a factor of 2.

3. ENTRY OF COSMIC RAYS INTO MOLECULAR CLOUD CORES

Strong magnetic fields can affect the trapping and production of ^{10}Be nuclei in molecular cloud cores in several ways. As the previous section has shown, strong magnetic fields can retard collapse, allowing more time for ^{10}Be cosmic rays to be produced or trapped in the cloud core. Strong magnetic fields can also focus cosmic rays into cloud cores, since cosmic rays are constrained to propagate along magnetic field lines. On the other hand, strong magnetic fields can also exclude many cosmic rays from entering cloud cores, by magnetic mirroring due to the field lines converging in the cloud core. In this section we consider the effects of magnetic focusing and mirroring.

Magnetic field strengths in the interstellar medium (ISM), the source region of the GCRs we measure, are commonly assumed to lie in the range $B_{\text{ISM}} \approx 4\text{--}7 \mu\text{G}$ (Chandrasekhar & Fermi 1953; Zweibel & Heiles 1997). The interstellar GCR flux would be in equipartition with a magnetic field if its strength was $7 \mu\text{G}$ (Webber 1998). We adopt a conservative value of $B_{\text{ISM}} = 4 \mu\text{G}$. Our final computed $^{10}\text{Be}/^9\text{Be}$ ratios vary by less than 10% over the range $B_{\text{ISM}} = 4\text{--}7 \mu\text{G}$. The ratio between B in the cloud core and B_{ISM} determines the degree of magnetic focusing. Cosmic rays are constrained to gyrate around magnetic field lines, so for the same number of cosmic rays per length of field line, the flux of cosmic rays per area must be proportional to the density of magnetic field lines per area, which is simply B . Defining $\chi \equiv B/B_{\text{ISM}}$, the GCR flux in the molecular cloud core must be a factor of χ greater than the ISM flux.

On the other hand, magnetic mirroring prevents many cosmic rays from entering the cloud core. As a cosmic ray propagates in the ISM with pitch angle α_{ISM} and speed v_{ISM} , its velocity along the magnetic field is $v_{\parallel} = v_{\text{ISM}} \cos \alpha$, and its velocity of gyration around the magnetic field line is $v_{\perp} = v_{\text{ISM}} \sin \alpha$. As the cosmic ray propagates, two quantities are conserved: kinetic energy, proportional to $v_{\perp}^2 + v_{\parallel}^2$, and the magnetic moment, $\propto v_{\perp}^2/B$. If the cosmic ray propagates into a region of high B , v_{\perp}^2 must increase as well to conserve the magnetic moment. To conserve the kinetic energy, v_{\parallel}^2 must therefore decrease, and the pitch angle must grow closer to 90° . By the time a cosmic ray has reached a region with $B = \chi B_{\text{ISM}}$, its new pitch angle α is given by

$$\cos^2 \alpha = 1 - \chi + \chi \cos^2 \alpha_{\text{ISM}}. \quad (3)$$

From this equation it is evident that $\cos^2 \alpha$ will be negative unless $\cos^2 \alpha_{\text{ISM}} > 1 - 1/\chi$. Physically, unless a cosmic ray starts in the ISM with a small enough pitch angle, it will be bounced out of regions with $B = \chi B_{\text{ISM}}$. This affects the number of cosmic rays that can enter a molecular cloud core.

Keeping all else constant, magnetic mirroring of cosmic rays reduces their flux in a molecular cloud core more than magnetic focusing increases it. The angle-integrated GCR flux \mathcal{F}_{cr} in the ISM is

$$\mathcal{F}_{\text{cr}}(\text{ISM}) = (2)2\pi \int_0^{+\pi/2} F_{\text{cr}} \sin \alpha_{\text{ISM}} d\alpha_{\text{ISM}}, \quad (4)$$

where the factor of 2 accounts for integration from 0 to $\pi/2$ at one surface of the cloud, plus integration from $\pi/2$ to π at the other surface. Because the GCR flux in the ISM is isotropic (e.g., Chandran 2000), $\mathcal{F}_{\text{cr}} = 4\pi F_{\text{cr}}$, where F_{cr} is the GCR flux in the ISM per steradian. After entering the molecular cloud core, the distribution of pitch angles is changed. Multiplying by χ to account for magnetic focusing and using equation (3) to convert from an integral over the ISM pitch angle α_{ISM} to an integral over the pitch angle α in the cloud core, we find the total angle-integrated flux in the cloud core to be

$$\mathcal{F}_{\text{cr}}(\text{core}) = 4\pi \int_0^{+\pi/2} \frac{\chi \cos \alpha}{(\chi^2 - \chi + \chi \cos^2 \alpha)^{1/2}} F_{\text{cr}} \sin \alpha d\alpha. \quad (5)$$

Performing the integral, we find

$$\mathcal{F}_{\text{cr}}(\text{core}) = \left[\chi - (\chi^2 - \chi)^{1/2} \right] 4\pi F_{\text{cr}}. \quad (6)$$

If $\chi = 1$, then the angle-integrated fluxes in the cloud core equal those in the ISM. In the limit $\chi \gg 1$, $\mathcal{F}_{\text{cr}}(\text{core}) = 2\pi F_{\text{cr}}$, so that magnetic focusing and mirroring together are seen to reduce the total angle-integrated GCR flux by a factor of 2 inside the cloud core. However, we note that the angle-integrated flux is *not* the most relevant input to calculations of the GCR contributions to ^{10}Be in the cloud core.

Instead, we must calculate the angle-integrated product of flux times the column density of cloud core gas that GCRs interact with before they pass through the cloud core. This is important, for example, in determining the number of spallation reactions that occur. The total column density through the cloud core is fixed at Σ_{\perp} , but the column density passed through by a cosmic ray with pitch angle α is larger, $\Sigma_{\perp} / \cos \alpha$. The angle-integrated product of GCR flux times the column density is then

$$4\pi \int_0^{+\pi/2} \frac{\chi \cos \alpha}{(\chi^2 - \chi + \chi \cos^2 \alpha)^{1/2}} F_{\text{cr}} \frac{\Sigma_{\perp}}{\cos \alpha} \sin \alpha d\alpha. \quad (7)$$

We define a new quantity A such that the above integral is $A(E)\Sigma_{\perp}4\pi F_{\text{cr}}(E)$. In that case,

$$A(E) = \frac{1}{\Sigma_{\perp}} \int_0^{+\pi/2} \frac{\chi \cos \alpha}{(\chi^2 - \chi + \chi \cos^2 \alpha)^{1/2}} \frac{\Sigma_{\perp}}{\cos \alpha} \sin \alpha d\alpha. \quad (8)$$

This expression assumes all GCRs pass through the cloud core.

Not all cosmic rays will pass through the cloud core, however. For pitch angles near 90° , $\Sigma_{\perp} / \cos \alpha$ will exceed the stopping length $\Sigma_{\text{stop}}(E)$ of the cosmic ray, the column density through which a cosmic ray of energy E can travel before it loses all its kinetic energy to interactions with the gas (as defined in § 5.1). In equation (8) above, one should replace $\Sigma_{\perp} / \cos \alpha$ with $\min(\Sigma_{\text{stop}}(E), \Sigma_{\perp} / \cos \alpha)$. Because $\Sigma_{\text{stop}}(E)$ is a function of the cosmic ray's energy E , A is in general a

function of E . Defining $\tau(E) = \Sigma_{\perp} / \Sigma_{\text{stop}}(E)$, we can calculate $A(E)$ in two regimes. If $\tau(E) \geq 1$ (meaning that *all* GCRs at that energy are stopped by the cloud core), then

$$A(E) = \frac{\chi}{\tau(E)} \left[1 - (1 - 1/\chi)^{1/2} \right]. \quad (9)$$

For very low energy GCRs (~ 1 MeV nucleon $^{-1}$), $\tau(E) \gg 1$ and $A(E) \ll 1$. If $\tau(E) \leq 1$ (meaning that only those GCRs with pitch angles close enough to 90° are stopped),

$$A(E) = \frac{\chi^{1/2}}{\tau(E)} \left[\left(\chi - 1 + \tau(E)^2 \right)^{1/2} - (\chi - 1)^{1/2} \right] + \chi^{1/2} \left[+ \sinh^{-1} \left(1/(\chi - 1)^{1/2} \right) - \sinh^{-1} \left(\tau(E)/(\chi - 1)^{1/2} \right) \right]. \quad (10)$$

For $\tau(E) \ll 1$, $A(E)$ approaches $\chi^{1/2} \sinh^{-1}(\chi - 1)^{-1/2}$, which is typically in the range 1.0–1.5 for $\chi \gtrsim 1.5$. Using the values of χ typical in our calculations, $A(E) \approx 1.1$ at the moderately high energies for which $\tau(E) \ll 1$. The case of trapping of cosmic rays is not related to a geometric factor alone and is discussed in § 5.1, but the expression for $A(E)$ allows us to compute the amount of gas irradiated by incoming GCRs. It should be added that if the magnetic field were turbulent and inhomogeneous on scales $\ll 1$ pc, magnetic inhomogeneities could serve as scattering centers and cause cosmic rays to scatter in pitch angle or suffer multiple bounces within the cloud core. These effects would increase the column density of gas that cosmic rays would interact with, enhancing both spallation by and trapping of cosmic rays.

4. COSMIC-RAY FLUX IN THE SOLAR NEBULA

GCRs affect the abundance of ^{10}Be nuclei in the solar nebula in two ways. First, GCRs (usually protons or α -particles) can spall nucleons off ambient C, N, or O nuclei, leaving ^{10}Be nuclei as residues. Because the momentum exchanged in such spallation reactions is small (§ 5.2), the newly created ^{10}Be nuclei remain part of the molecular cloud core gas and eventually enter the solar nebula. Ambient H nuclei can also spall GCR CNO nuclei, also creating ^{10}Be . These nuclei retain the momentum of the original C, N, or O GCR, and most of them escape the cloud core, so we neglect these “inverse” reactions. Inverse reactions throughout the interstellar medium, however, do create abundant ^{10}Be GCRs. Those ^{10}Be GCRs of low energy can lose enough kinetic energy (as they ionize ambient gas molecules) that they can become trapped in the molecular cloud core. Trapping of ^{10}Be GCRs in the cloud core is the second way in which GCRs affect the solar nebula abundance of ^{10}Be and, we show, is the dominant contribution.

GCR fluxes of protons, α -particles, and ^{10}Be nuclei are necessary inputs to calculations of spallation and trapping. The proton and α -fluxes must be specified over the energy range 30 to ~ 3000 MeV nucleon $^{-1}$ at which spallation reactions occur. The thresholds for spallation reactions lie near 30 MeV nucleon $^{-1}$, while fewer than 10% of GCRs have energies above a few GeV nucleon $^{-1}$. On the other hand, the GCR ^{10}Be fluxes must be specified only at energies $\lesssim 10^2$ MeV nucleon $^{-1}$, since GCRs at higher energies will not be trapped in the cloud core. These fluxes are reasonably well established for the environment near the present-day Sun, as we discuss in § 4.2. In § 4.2, we discuss the extrapolation of these

quantities to conditions in the molecular cloud core from which our solar system formed 4.5 Gyr ago.

4.1. GCR Flux in Today's Solar Neighborhood

Until the *Voyager* spacecraft cross the heliopause in the coming decades no direct measurements of the interstellar GCR flux will be possible. Interstellar GCRs lose several times 10^2 MeV nucleon⁻¹ of kinetic energy as they propagate “upstream” against the solar wind. Low-energy GCRs are therefore excluded entirely from the inner solar system, and we have no direct information about the flux of low-energy interstellar GCRs. Models are used instead to predict their flux, usually by assuming a power-law spectrum of initial GCR energies followed by propagation through the Galaxy under various assumptions (e.g., “leaky box” models). These models indicate that for GCRs with energies $\lesssim 1$ GeV nucleon⁻¹, losses of kinetic energy due to ionization of ambient gas are a significant effect (and losses of energy due to nuclear reactions are not; Nath & Biermann 1994). Finally, the effect of the solar wind on the entry of GCRs into the solar system is accounted for (“modulation”), for comparison with spacecraft data.

Notwithstanding the many uncertainties in backing out interstellar GCR fluxes from spacecraft data, reasonable convergence in the derived fluxes exists across all models. Mori (1997) showed that all models in the literature were within a factor of 2 of the median flux at energies below 1 GeV, and the agreement was even better at higher energies. We use the derived flux of Webber (1998), which relies on *Pioneer* and *Voyager* measurements at 80 AU (which minimizes solar modulation). Over the energy range $100 \text{ MeV} \lesssim E \lesssim 3000 \text{ MeV}$, the GCR proton flux in Figure 2 of Webber (1998) is well described as

$$F_p = 1.15 \times 10^5 (E + 750)^{-2.6} \text{ cm}^{-2} \text{ s}^{-1} \text{ sr}^{-1} (\text{MeV nucleon}^{-1})^{-1}, \quad (11)$$

where E is the kinetic energy per nucleon in units of MeV. The GCR α -flux is identical except for the coefficient, which is 7.7×10^3 . These derived fluxes are consistent within factors of 2 of the median flux of Mori (1997) and the spectra derived by Ip & Axford (1985), Prantzos et al. (1993b), and Lemoine et al. (1998). As we show below, spallation reactions contribute only about 20% of the solar nebula ¹⁰Be nuclei, so uncertainties of even a factor of 2 in the spallation rates will lead to uncertainties of 10% at most in our predicted ¹⁰Be/⁹Be ratio of the solar nebula.

Fortunately, the GCR proton flux below $100 \text{ MeV nucleon}^{-1}$, to which the low-energy ¹⁰Be flux is tied, is much less uncertain. Particles with energies \lesssim a few times $100 \text{ MeV nucleon}^{-1}$ lose kinetic energy at a relatively much greater rate as they ionize ambient gas molecules. Because of this, the low-energy tail of the interstellar GCR spectrum is predicted by many groups to be essentially flat (Lerche & Schlickeiser 1982; Ip & Axford 1985; Prantzos, Casse, & Vangioni-Flam 1993a; Webber 1998; Lemoine et al. 1998). Each of these groups derives a proton flux from a few 100 MeV of $\approx 2.5 \times 10^{-3} \text{ cm}^{-2} \text{ s}^{-1} \text{ sr}^{-1} \text{ MeV}^{-1}$, to within a few tens of percent. This flux is about 35% lower than would be suggested by an extrapolation of equation (11) to low energies.

Rates at which GCR ¹⁰Be nuclei are trapped in the cloud core are proportional to the fluxes of low-energy ($\ll 100 \text{ MeV nucleon}^{-1}$) GCR ¹⁰Be nuclei. Typically spacecraft measure the GCR C flux, the ratio of the Be flux to the C flux, and the ratio of the ¹⁰Be flux to the Be flux, at various energies. Webber

(1998) inferred a combined flux of GCR C, N, and O nuclei that decreases with decreasing energy, from $\approx 7.5 \times 10^{-6} \text{ cm}^{-2} \text{ s}^{-1} \text{ sr}^{-1} (\text{MeV nucleon}^{-1})^{-1}$ at $100 \text{ MeV nucleon}^{-1}$ to about half that value at $10 \text{ MeV nucleon}^{-1}$. C nuclei make up 45% of the combined CNO flux at $620 \text{ MeV nucleon}^{-1}$ (Engelmann et al. 1990) and the range $40\text{--}450 \text{ MeV nucleon}^{-1}$ (Duvernois & Thayer 1996), so we infer a low-energy C flux in the range $(1.7\text{--}3.4) \times 10^{-6} \text{ cm}^{-2} \text{ s}^{-1} \text{ sr}^{-1} (\text{MeV nucleon}^{-1})^{-1}$. Since most of the trapped GCRs have energies $\lesssim 15 \text{ MeV nucleon}^{-1}$, we conservatively adopt the lower value of the C flux. This may be an underestimate; Ip & Axford (1985) infer a C flux at $100 \text{ MeV nucleon}^{-1}$ in the range $(10\text{--}30) \times 10^{-6} \text{ cm}^{-2} \text{ s}^{-1} \text{ sr}^{-1} (\text{MeV nucleon}^{-1})^{-1}$, an order of magnitude higher.

After the fluxes of GCR C, N, and O nuclei are determined, the fluxes of Be and ¹⁰Be nuclei are readily determined. The Be/C ratios measured by spacecraft are Be/C = 0.078 and Be/CNO = 0.035, with 5% uncertainty, at $620 \text{ MeV nucleon}^{-1}$ (Engelmann et al. 1990); Be/C = 0.070 and Be/CNO = 0.031, with 6% uncertainty, at $40\text{--}450 \text{ MeV nucleon}^{-1}$ (Duvernois & Thayer 1996); and Be/C = 0.0536, with 2% uncertainty, at $40\text{--}105 \text{ MeV nucleon}^{-1}$ (Ferrando et al. 1991). Webber, Lukasiak, & McDonald (2002) combine these data with newer 1997 *Voyager* data to find Be/C = 0.0553, with about 4% uncertainty. For this last set of data, the solar modulation was quite low (270 MV), and we adopt this ratio and uncertainty. The same Webber et al. (2002) results indicate that Be cosmic rays are $57.4\% \pm 4.3\%$ ⁷Be, $38.3\% \pm 3.7\%$ ⁹Be, and $4.2\% \pm 1.1\%$ ¹⁰Be. The large errors on the ¹⁰Be fraction stem from the small number (14) of detections. Webber et al. (2002) also used a propagation calculation to model the fluxes of all Li, Be, and B isotopes. They find excellent agreement with the measured fluxes, so we adopt their predicted value for the ¹⁰Be/Be ratio, 4.9%. This value is consistent with other measurements of the ¹⁰Be/Be ratio reported by Lukasiak et al. (1994): $4.3\% \pm 1.5\%$ measured by *Voyager 1* and *2* at $35\text{--}113 \text{ MeV nucleon}^{-1}$, $3.9\% \pm 1.4\%$ measured by *IMP 7/8* at $46\text{--}135 \text{ MeV nucleon}^{-1}$, and $6.4\% \pm 1.5\%$ measured by *ISEE 3* at $60\text{--}185 \text{ MeV nucleon}^{-1}$.

Now the ¹⁰Be flux and its uncertainty are readily found since the measured ¹⁰Be/C ratio is 2.70×10^{-3} , to within 30%. Combining all the above, the present-day GCR flux of ¹⁰Be nuclei at energies $\lesssim 100 \text{ MeV nucleon}^{-1}$ is

$$F_{10\text{Be}} \approx 4.6 \times 10^{-9} \text{ cm}^{-2} \text{ s}^{-1} \text{ sr}^{-1} (\text{MeV nucleon}^{-1})^{-1}. \quad (12)$$

While the C flux could be much higher than we have assumed (see Ip & Axford 1985), we estimate that it is unlikely to be many tens of percent lower than our assumed value. The dominant source of uncertainty appears to be the ¹⁰Be/Be ratio, which leads us to estimate a total uncertainty of about 30% in the ¹⁰Be flux.

4.2. GCR Flux in the Sun's Molecular Cloud Core

Key to determining the abundance of ¹⁰Be in CAIs formed at the beginning of the solar system is extrapolating the present-day GCR flux to that in the Sun's molecular cloud core of 4.5 Gyr ago. The spatial variation of the GCR flux in the Galaxy today is apparently small, and the GCR flux impinging on the solar system is representative of the Galaxy at 8.5 kpc galactocentric distance. This result comes from comparisons of the solar system GCR flux with the ionization rates inferred for various molecular cloud cores. Webber (1998) derived a cosmic-ray ionization rate from the GCR flux

at the solar system of $\zeta \approx (3-4) \times 10^{-17} \text{ s}^{-1}$. This is to be compared with the ionization rates inferred from the chemistry of seven massive star-forming cores, which were $(2.6 \pm 1.8) \times 10^{-17} \text{ s}^{-1}$ and in a tight range (van der Tak & van Dishoeck 2000). Other fits to the chemistry in a larger sample of low-mass star-forming cores are consistent with a uniform $\zeta = 5 \times 10^{-17} \text{ s}^{-1}$ (Williams et al. 1998) or an average ζ near this value. There is little evidence that the GCR flux varies within the nearest few 100 pc from the Sun. From a theoretical standpoint, a uniform GCR flux is expected because cosmic rays diffuse several 100 pc before they escape the Galaxy or are thermalized (Yanasak et al. 2001). Only on scales greater than 1 kpc are even factor-of-2 variations in the GCR fluxes inferred, from the chemistry in cloud cores (van der Tak & van Dishoeck 2000) and from gamma-ray observations (Hunter et al. 1997). The variations of a factor of 10 in the GCR flux argued for by Caselli et al. (1998) appear to be sensitive to assumptions about elemental depletions, and the same methodology was found by Williams et al. (1998) to be consistent with a uniform GCR flux. The GCR fluxes measured by spacecraft are typical for the Galaxy, and the fluxes 4.5 Gyr ago were probably equally spatially homogeneous.

Supernova shocks are the probable mechanism by which GCRs are accelerated to MeV energies. The model of Meyer, Drury, & Ellison (1997) and Ellison, Drury, & Meyer (1997) advocates that supernova shocks both injected ions (i.e., accelerated them to 0.1 MeV nucleon⁻¹ energies) and accelerated them to higher energies of 1–10⁹ MeV nucleon⁻¹. The mechanism preferentially injects high-rigidity ions (with high mass-to-charge ratios A/Q) and for those ions of volatile elements explains the observed correlation between rigidity and abundance in GCRs. Nonvolatile (condensation temperature $\gtrsim 400$ K) elements are locked in dust grains, which behave as high-rigidity ions until they are sputtered and destroyed. These elements are efficiently injected and are equally overabundant in GCRs, explaining the GCR fluxes of Mg, Fe, Si, etc. The only exceptions to this trend are ¹²C and ²²Ne and ¹⁶O, which are enhanced by even larger than expected values. However, these are the specific isotopes ejected in a Wolf-Rayet outflow, a stage that a known fraction of supernovas go through. Meyer et al. (1997) and Ellison et al. (1997) find consistency between the number of supernovas that could accelerate their own ²²Ne-¹²C-¹⁶O-rich material and the abundances of these isotopes in the GCR flux.

Having identified an acceleration mechanism, then, we can extrapolate to 4.5 Gyr ago and compute the composition of GCRs at the birth of the solar system. Since both protons and α -particles are accelerated from the gas, their ratios do not change. On the other hand, ¹⁰Be GCRs are produced only when CNO GCRs collide with ambient gas and are spalled. The metallicity of the Galaxy 4.5 Gyr ago was about 0.7 times today's metallicity (Dwek 1998), so the ratio of N nuclei to protons in GCRs was about 70% of today's value. On the other hand, 80% of the C nuclei in GCRs we assume are accelerated out of the supernovas' own Wolf-Rayet wind material, so the ratio of C nuclei to protons in GCRs is essentially unchanged. Relative to the combined CNO flux in GCRs today, the proportions of (low energy) C, N, and O in GCRs today are 0.45:0.10:0.45 (Duvernois & Thayer 1996, respectively; Engelmann et al. 1990). On the same scale, we infer fluxes of C, N, and O nuclei 4.5 Gyr ago of 0.42:0.07:0.32, respectively. Multiplying these fluxes by the appropriate cross sections for production of ¹⁰Be by spallation

(§ 5.2) we estimate that relative to the GCR proton flux the ¹⁰Be GCR flux 4.5 Gyr ago was about 83% of today's value.

Using this ¹⁰Be/proton ratio derived for 4.5 Gyr ago, we can derive the ¹⁰Be flux if we fix the GCR proton flux 4.5 Gyr ago. The GCR proton flux is directly proportional to the supernova rate over the previous ≈ 15 Myr (Yanasak et al. 2001), and the supernova rate is proportional to the star formation rate (SFR) with a lag of $\sim 10^7$ yr, so the GCR flux closely follows the SFR. Some observations can constrain the GCR flux over Galactic history, and some observations constrain the SFR over Galactic history. Both types of observation suggest that ψ , the GCR flux 4.5 Gyr ago relative to today's flux, was in the range $1.5 \lesssim \psi \lesssim 2.9$.

Studies of Li, Be, and B abundances in the stellar atmospheres constrain the GCR flux over Galactic history directly (since these elements are produced by GCR spallation). In the model of Vangioni-Flam et al. (1990), their model V, with $\psi = 1.5$ (from their Table 1), best fits the data. Their model S also is a reasonable fit, with $\psi = 2.0$. Valle et al. (2002) showed that the most recent 5 Gyr of Galactic chemical evolution are adequately approximated by a simple closed-box model (see their Fig. 5) such that the SFR varies as $\exp(-t/4.2 \text{ Gyr})$ (their eq. [18]), indicating that $\psi = 2.9$. Finally, in their model of Li, Be, and B production, Prantzos et al. (1993a) also inferred an increase in GCR flux in the past (but they used a changing GCR spectrum, precluding a determination of ψ).

Higher GCR fluxes in the past are also indicated by the ages of G dwarfs. Most of these models find evidence for a burst of star formation 4–5 Gyr ago (Twarog 1980; Scalo, Barry, & Sneden 1987; Barry 1988; Marsakov, Shevelev, & Suchkov 1990; Meusinger 1991; Rocha-Pinto et al. 2000). The recent models of Rocha-Pinto et al. (2000) suggest $\psi \approx 1.5-2.2$, depending on how outliers in the data are rejected. Finally, Galactic chemical evolution models also indicate $\psi \approx 2$. Dwek (1998) found $\psi = 2.2$ (his Fig. 5), and Chang, Shu, & Hou (2002) found $\psi = 2.7$ in their preferred model A, or $\psi = 2.3$ in their model E (see their Fig. 11). Altogether a range $1.5 \lesssim \psi \lesssim 2.9$ is inferred from the various models. We adopt an average of 2.2 and estimate an uncertainty of several tens of percent.

On top of these uncertainties in ψ , we add that the models constructed above all necessarily put stars of different ages into different age bins. Typically each bin is an average of conditions over 400 Myr, and spikes in the SFR over much shorter timescales would not be inferred from the observations (Rocha-Pinto et al. 2000). Another caveat is that the Sun might not have formed at 8.5 kpc galactocentric distance (where it is now); because of the Sun's high metallicity it has been suggested that the Sun formed at 6.6 ± 0.9 kpc (Wielen, Fuchs, & Dettbarn 1996). The SFR at 6.6 kpc is today about a factor of 2 higher than the flux at 8.5 kpc (see Fig. 5 of Chang et al. 2002). We adopt $\psi = 2.0$ and associate with it an uncertainty on the order of 50%. This uncertainty is the largest source of uncertainty in determining the GCR fluxes. To get the fluxes of 4.5 Gyr ago, we multiply the GCR proton flux by ψ and the ¹⁰Be flux by 0.83ψ .

5. GCR CONTRIBUTIONS TO SOLAR NEBULA BERYLLIUM 10

5.1. Trapping of Beryllium 10 Cosmic Rays

Trapping of cosmic rays in molecular cloud cores is achieved once the cosmic rays lose enough kinetic energy to ionize the gas and are thermalized. Below 100 MeV nucleon⁻¹, losses due to ionizing gas molecules far outweigh other losses

such as nuclear interactions (Nath & Biermann 1994). The energy loss rate due to ionizations of a particle of atomic mass A and charge ze moving at speed βc (where c is the speed of light) through a gas is

$$-\left(\frac{dE}{dx}\right) = 1.18 \frac{4\pi e^4 Z z^2}{m_e c^2 M \beta^2} \left[\log \frac{2m_e c^2 \beta^2}{I(1-\beta^2)} - \beta^2 \right] \quad (13)$$

(Bethe 1933), where $Z = 1$, $M = m_H$, and $I = 20.0$ eV for pure hydrogen gas (Umebayashi & Nakano 1981), x represents a column density (in g cm^{-2}), and other constants have their usual meanings. The additional factor of 1.18 in the energy loss rate accounts for additional losses to helium atoms (Ramaty, Kozlovsky, & Lingenfelter 1996). The term in brackets in equation (13) is weakly dependent on velocity β , but the β^{-2} -term multiplying it means that low-energy cosmic rays lose energy at a much faster rate than do high-energy cosmic rays. The total kinetic energy of the particle is

$$E = (\gamma - 1) A m_H c^2, \quad (14)$$

where $\gamma = (1 - \beta^2)^{-1/2}$. From this one can derive an approximate ‘‘stopping length,’’ a representative column density of gas a cosmic ray must pass through before it is stopped:

$$l_{\text{stop}} \approx \frac{E}{-dE/dx} \approx 2600 \frac{A}{z^2} \frac{(\gamma - 1)\beta^2}{10.84 + \ln(\beta^2 \gamma^2) - \beta^2} \text{ g cm}^{-2}. \quad (15)$$

For example, the approximate stopping length of ^{10}Be nuclei with energies of 10 MeV nucleon $^{-1}$ is ≈ 0.052 g cm^{-2} .

However, a more careful calculation must consider the changing rate of energy loss as the cosmic ray is slowed. By equation (13), the energy loss rate varies inversely with energy, so particles are stopped ever more effectively as they lose energy. We calculate a more exact stopping length $\Sigma_{\text{stop}}(E)$ by assuming cosmic rays begin with energy E , integrating over a small column density $\delta\Sigma$, computing a new energy and energy loss rate by equation (13), and continuing to integrate over Σ until the cosmic-ray energy drops below 1 MeV nucleon $^{-1}$, at which point it is assumed trapped. The total column density of gas that the cosmic ray of initial energy E needs to traverse before it is trapped is the stopping length $\Sigma_{\text{stop}}(E)$, which can be significantly lower than l_{stop} for $E \lesssim 100$ MeV nucleon $^{-1}$. For example, for 10 MeV nucleon $^{-1}$ ^{10}Be cosmic rays, $\Sigma_{\text{stop}} \approx 0.003$ g cm^{-2} . All ^{10}Be cosmic rays with energies less than 10 MeV nucleon $^{-1}$ are stopped by 0.003 g cm^{-2} of molecular cloud core gas.

In practice, we turn the problem around and define a critical energy per nucleon E_c for each column density Σ that the GCR passes through such that all ^{10}Be GCRs with energies $E < E_c$ are thermalized by that column density Σ , while all ^{10}Be GCRs with $E > E_c$ can pass through it. The number of ^{10}Be GCRs trapped per time is found by integrating over the ^{10}Be GCR spectrum up to energies per nucleon of $E_c(\Sigma)$. Because $\Sigma = \Sigma_{\perp} / \cos \alpha$ depends on the pitch angle, integration must also be taken over all pitch angles inside the cloud. These in turn are related to the pitch angles outside the cloud, analogous to the calculations in § 3. The rate at which ^{10}Be GCRs are trapped per unit area of the cloud core is then found:

$$F_{\text{trap}} = (2)2\pi \int_0^{\pi/2} \frac{\chi \cos \alpha}{(\chi^2 - \chi + \chi \cos^2 \alpha)^{1/2}} \times \int_{1 \text{ MeV/n}}^{E_c(\Sigma_{\perp}/\cos \alpha)} F_{\text{Be10}}(E) dE \sin \alpha d\alpha. \quad (16)$$

Having found F_{trap} , we can easily compute the rate at which ^{10}Be nuclei are added to the cloud core, per ^9Be nucleus:

$$\dot{R}_{\text{trap}} \equiv \frac{d}{dt} \left(\frac{^{10}\text{Be}}{^9\text{Be}} \right)_{\text{trap}} = \left(x_{\text{Be9}} \frac{\Sigma_{\perp}(t)}{1.4 m_H} \right)^{-1} F_{\text{trap}}. \quad (17)$$

The factor dividing F_{trap} is the number of ^9Be nuclei per unit area, and F_{trap} is the number of new ^{10}Be nuclei per unit area per time. Contributions to ^{10}Be are highest when Σ_{\perp} is small, so that the collecting area (for ^{10}Be GCRs) is large relative to the number of diluting ^9Be nuclei. On the other hand, if Σ_{\perp} is too small, then most ^{10}Be nuclei will pass through it. There is a tendency for trapping to be optimal at column densities $\Sigma_{\perp} \sim 0.01$ g cm^{-2} , which is exactly comparable to the column densities of actual molecular cloud cores early in their evolution.

5.2. Direct Spallation Reactions

Magnetic mirroring and focusing and pitch angle redistribution likewise affect the flux of GCR protons and α -particles entering molecular cloud cores. For typical Σ_{\perp} , GCR protons and α -particles with energies \lesssim tens of MeV per nucleon are trapped in the cloud core, and GCRs with pitch angles arbitrarily close to 90° will always be trapped even if Σ_{\perp} is small. Integrating over all pitch angles, the average column density of cloud core gas that GCR protons and α -particles of energy per nucleon E interact with is $\Sigma_{\perp} A(E)$, where $A(E)$ is the geometric factor derived in § 3. Before a GCR passes through a cloud core or is stopped in the cloud core, it has time to initiate a nuclear spallation reaction.

Spallation reactions produce ^{10}Be nuclei in molecular cloud cores when protons or α -particles collide with C, N, or O nuclei and strip nucleons off them. This process can involve either ‘‘direct reactions,’’ energetic protons or α -particles (kinetic energies $\gtrsim 30$ MeV nucleon $^{-1}$) striking stationary CNO nuclei, or ‘‘inverse reactions,’’ energetic CNO GCRs colliding with ambient H or He nuclei. In fact only direct reactions contribute significantly because when a cosmic-ray CNO nucleus is spalled the newly created ^{10}Be nucleus retains nearly the entire momentum of the CNO cosmic ray. The ^{10}Be nucleus is therefore likely to escape the cloud core. On the other hand, when a GCR proton or α -particle spalls an ambient CNO nucleus, the newly created ^{10}Be nucleus has a small momentum per nucleon $\lesssim 100$ MeV/ c . The ^{10}Be nuclei produced in this way are easily retained by the cloud core.

Empirical formulas describing the final momentum of a residue nucleus created by spallation of a larger nucleus have been summarized by Morrissey (1989). The final momentum is the sum of two momentum vectors. One is the average momentum that the residue nucleus acquires along the direction the cosmic ray was traveling. This longitudinal momentum transfer has magnitude $P_{\parallel} \approx (8 \text{ MeV}/c)(\Delta A)$, where ΔA is the number of nucleons lost from the target nucleus to produce the residue [e.g., $\Delta A = 6$ in the reaction $p(^{16}\text{O}, x)\text{Be}$]. To this is added a recoil momentum. The orientation of the recoil momentum is randomly distributed. The magnitude of the recoil momentum, when projected along any

axis, follows a Gaussian distribution with zero mean and width $P_{\text{rms}} \approx (150 \text{ MeV}/c)(\Delta A)^{1/2}$. The recoil momentum is much more significant to the final kinetic energy of the ^{10}Be nucleus than is the longitudinal momentum.

Loss of newly created ^{10}Be nuclei from the cloud core is easily calculated using these empirical formulas. We assume that direct spallation reactions occur with a uniform distribution throughout the cloud core (since the stopping lengths of GeV nucleon $^{-1}$ protons and α -particles doing the spallation are so much larger than the cloud core column density). As a worst-case scenario, we use $\Delta A = 6$ for both the longitudinal and recoil momenta. We conservatively assume that the longitudinal momentum transfer is aligned along the direction of the magnetic field and integrate over the Gaussian distribution of possible recoil momenta and over all orientations of the recoil momentum. We then propagate the ^{10}Be nuclei so produced, accounting for the loss of kinetic energy to gas molecule ionizations according to equation (13). If the ^{10}Be nucleus reaches a cloud core surface with a kinetic energy greater than 1 MeV nucleon $^{-1}$, it is considered to escape the cloud core; otherwise it has been trapped. In this way we find that even at low column densities ($\Sigma_{\perp} = 0.005 \text{ g cm}^{-2}$) over 98.3% of all ^{10}Be nuclei produced by direct spallation reactions will remain trapped in the core. We assume that *all* ^{10}Be nuclei produced by direct spallation reactions are trapped in the core. By the same token, the momentum transferred to a GCR CNO nucleus during an inverse reaction is small, and the resulting ^{10}Be nucleus is likely to retain the ~ 1 GeV nucleon $^{-1}$ kinetic energy of the spalled GCR CNO nucleus and escape the cloud core.

For the cross sections of the ^{10}Be -producing direct spallation reactions between CNO nuclei and GCR protons, we have adopted the formulation of Yanasak et al. (2001), to which we refer the reader:

$$\sigma(E) = \begin{cases} \sigma_0(E/E_0)^x & \text{for } E < E_0, \\ \sigma_0 & \text{for } E \geq E_0. \end{cases} \quad (18)$$

The parameters for the reactions involving GCR protons are presented in Table 2. This formulation yields a quite satisfactory fit to the measured cross sections and is superior to interpolation of the data of Read & Viola (1984), which has been standard in studies of this type. For each of the reactions with GCR α -particles, we have adopted a constant cross section of 5 mb above threshold. Data are lacking for these reactions to provide energy-dependent cross sections, but 5 mb is typical (Read & Viola 1984). The threshold energies E_{th} we used for the various reactions are also tabulated.

Integration over energy of the product of GCR proton flux [times $4\pi A(E)$] and the spallation cross section $\sigma(E)$ for the reaction $^{12}\text{C}(p, x)^{10}\text{Be}$ yields the rate at which ^{10}Be nuclei are

produced per carbon nucleus in the cloud. Multiplying this by the factor $x_{\text{C}}/x_{\text{Be}9}$ yields the rate at which ^{10}Be nuclei are produced per ^9Be nucleus. Similar reactions hold for GCR α -particles and N and O nuclei. Summing over all possible reactions, the rate at which direct reactions increase the number of ^{10}Be nuclei per ^9Be nucleus in the molecular cloud core is then

$$\dot{R}_{\text{direct}} \equiv \frac{d}{dt} \left(\frac{^{10}\text{Be}}{^9\text{Be}} \right)_{\text{direct}} = \sum_i \sum_j y_i \frac{x_j}{x_{\text{Be}9}} \int_{E_{\text{th}}}^{10 \text{ GeV}/n} 4\pi F_p(E) \sigma_{ij}(E) A(E) dE, \quad (19)$$

where i stands for GCR protons or α -particles; y_i is the flux of GCR protons or α -particles relative to GCR protons (i.e., $y = 1$ for GCR protons, and $y = 0.065$ for GCR α -particles); j stands for C, N, or O; x_j is the abundance of molecular cloud core C, N, or O nuclei relative to hydrogen ($x_{\text{C}} = 2.45 \times 10^{-4}$, $x_{\text{N}} = 8.2 \times 10^{-5}$, $x_{\text{O}} = 4.90 \times 10^{-4}$; Anders & Grevesse 1989; Allende Prieto, Lambert, & Asplund 2001); $\sigma_{ij}(E)$ is the energy-dependent cross section for reactions between i and j ; and $F_{\text{cr}}(E)$ is the cosmic-ray proton flux. The factor $4\pi A(E)$ accounts for integration over the column density of gas that the GCR interacts with either as it passes through the cloud core ($\Sigma_{\perp}/\cos \alpha$) or before it is thermalized (Σ_{stop}), as well as the effects of magnetic focusing and mirroring and pitch angle redistribution.

6. RESULTS

Now that the rates at which trapping of ^{10}Be cosmic rays and GCR-induced spallation reactions increase the ^{10}Be abundance can be quantified, we can calculate the time evolution of the $^{10}\text{Be}/^9\text{Be}$ ratio. These rely on the time evolution of χ and Σ_{\perp} , for which we have used the results of the calculations of DM01 at the cloud core center, which should apply to the entire supercritical core. These results were sampled at 90 different times during the cloud core's evolution. Defining $R \equiv ^{10}\text{Be}/^9\text{Be}$, we calculate $R(t + \Delta t)$ in terms of $R(t)$ and the cosmic-ray contribution rates (\dot{R}) $_{\text{direct}}$ and (\dot{R}) $_{\text{trap}}$ based on the present-day GCR flux, as follows:

$$R(t + \Delta t) = R(t) \exp(-\Delta t/\tau) + \tau [1 - \exp(-\Delta t/\tau)] \times \frac{1}{2} \psi [\dot{R}_{\text{direct}}(t) + 0.83 \dot{R}_{\text{trap}}(t) + \dot{R}_{\text{direct}}(t + \Delta t) + 0.83 \dot{R}_{\text{trap}}(t + \Delta t)], \quad (20)$$

where $\tau = 2.18$ Myr is the mean life of ^{10}Be . For the production rates, the present-day GCR fluxes in the solar neighborhood are assumed and a solar composition of CNO nuclei in the gas is assumed. The factor ψ multiplying (\dot{R}) $_{\text{direct}}$ accounts for increased proton and α -flux 4.5 Gyr ago, and the factor 0.83ψ multiplying (\dot{R}) $_{\text{trap}}$ accounts for increased ^{10}Be flux 4.5 Gyr ago (§ 4.2).

The results of two simulations of the $^{10}\text{Be}/^9\text{Be}$ as a function of time are displayed in Figure 3, for molecular cloud cores with initial magnetic field strengths of 30 μG (as in DM01) and 15 μG (as is likely in actual cloud cores). We have assumed $\psi = 2.0$ and initialized both simulations with $^{10}\text{Be}/^9\text{Be} = 1 \times 10^{-4}$, although after several Myr most of the ^{10}Be initially present has decayed. Because the rate of ^{10}Be production by direct spallation reactions depends only very weakly on Σ_{\perp} [through $A(E)$] and on B (through χ), the ratio $^{10}\text{Be}/^9\text{Be}$ due to spallation reactions alone is nearly constant in time, at a level $\approx 2 \times 10^{-4}$. On the other hand, the contributions to the

TABLE 2
NUCLEAR REACTION PARAMETERS

Reaction	E_{th} (MeV)	σ_0 (mb)	E_0 (MeV nucleon $^{-1}$)	x
$^{12}\text{C}(p, x)^{10}\text{Be}$	27.4	3.79	1037	0.530
$^{14}\text{N}(p, x)^{10}\text{Be}$	32.1	1.75	671	0.715
$^{16}\text{O}(p, x)^{10}\text{Be}$	34.6	2.52	798	0.962
$^{12}\text{C}(\alpha, x)^{10}\text{Be}$	27.4	5.0	...	0.0
$^{14}\text{N}(\alpha, x)^{10}\text{Be}$	32.1	5.0	...	0.0
$^{16}\text{O}(\alpha, x)^{10}\text{Be}$	34.6	5.0	...	0.0

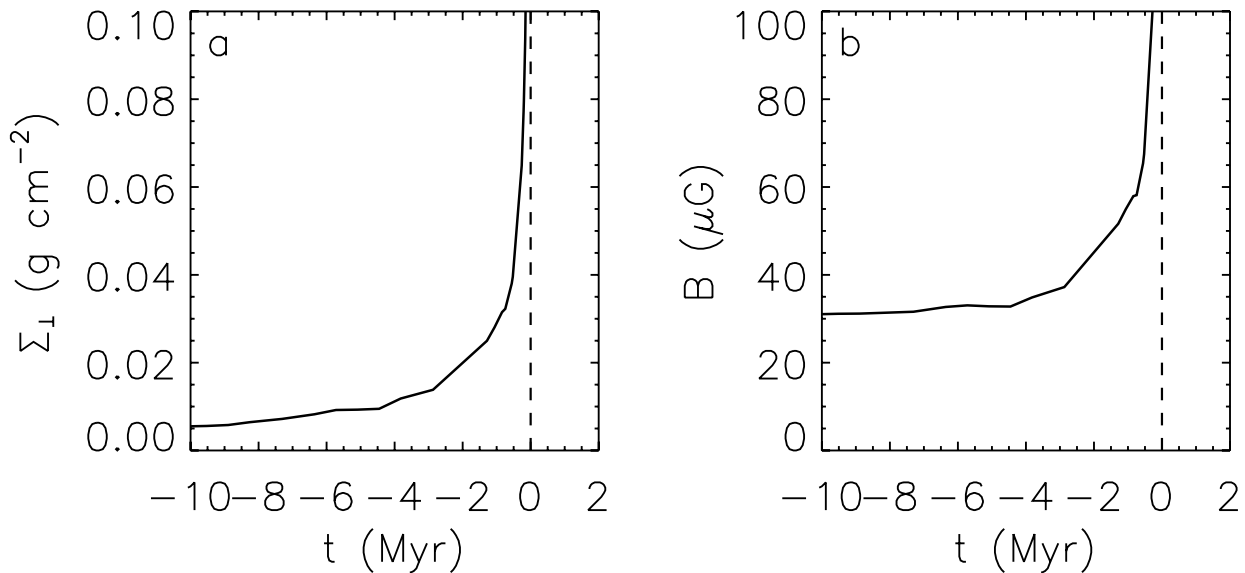


Fig. 1.—(a) Total column density of gas, Σ_{\perp} , through the molecular cloud core center; (b) magnetic field strength B at the cloud core center, both as functions of time t . Until a magnetically supercritical core forms, at $t \approx -0.4$ Myr, B varies by less than a factor of 2, while Σ_{\perp} increases by an order of magnitude. After the supercritical core forms, formation of a protostar takes only a few times 10^5 yr.

ratio $^{10}\text{Be}/^9\text{Be}$ from trapping of ^{10}Be cosmic rays are proportional to the collecting area of the cloud core but also inversely proportional to the mass of the cloud core (because more mass means more ^9Be nuclei to dilute the ratio). Therefore, as equation (16) shows, the rate of change of the $^{10}\text{Be}/^9\text{Be}$ due to trapping of ^{10}Be nuclei scales as $1/\Sigma_{\perp}(t)$, and ^{10}Be trapping makes its strongest contributions early in the cloud core's evolution. As seen in Figure 3, the $^{10}\text{Be}/^9\text{Be}$ ratio from trapping peaks at levels $\approx 1.45 \times 10^{-3}$ after an initial rise over a few ^{10}Be mean lives, then slowly declines as further contributions cease to keep up with the decay of ^{10}Be . The peak in the $^{10}\text{Be}/^9\text{Be}$ ratio occurs when $\Sigma_{\perp} \approx 0.004 \text{ g cm}^{-2}$, regardless of initial magnetic field strength B_0 . The nontrivial time evolution of the $^{10}\text{Be}/^9\text{Be}$ ratio demonstrates the need to use numerical simulations (such as those of DM01 used here) to determine $\Sigma_{\perp}(t)$ and $B(t)$.

Having established the time evolution of the $^{10}\text{Be}/^9\text{Be}$ ratio, we can at last say what the final $^{10}\text{Be}/^9\text{Be}$ ratio in the early solar system should have been. As Figure 1a illustrates, the final collapse to a protostar from which the DM01 calculations leave off takes only a few times 10^3 yr. Further evolution to a T Tauri star, with an accompanying protoplanetary disk, is expected to take place in less than a few times 10^5 yr. During this time, the $^{10}\text{Be}/^9\text{Be}$ can decrease at most 10%, and continued GCR contributions would lessen the decrease. We therefore can state, with about a factor of 3 uncertainty, that the $^{10}\text{Be}/^9\text{Be}$ ratio at the end of our calculations should be the same as the ratio recorded in CAIs. At the end of the case with $B_0 = 30 \mu\text{G}$, direct reactions yield $^{10}\text{Be}/^9\text{Be} = 2.2 \times 10^{-4}$, and trapping yields $^{10}\text{Be}/^9\text{Be} = 8.3 \times 10^{-4}$, for a combined value $^{10}\text{Be}/^9\text{Be} = 1.05 \times 10^{-3}$. This combined ratio (which assumed $\psi = 2.0$) is completely consistent with the values recorded by CAIs, $\approx 9 \times 10^{-4}$. Spallation reactions alone fail to match the CAI ratio by a factor of about 5, but trapping is in fact the dominant contribution from GCRs to the $^{10}\text{Be}/^9\text{Be}$ ratio.

Extrapolation to other initial magnetic field strengths B_0 is easily accomplished using the formulas for $\Sigma_{\perp}(t)$ and $B(t)$ described in § 2. Figure 2 shows the evolution for $B_0 = 15 \mu\text{G}$, and Figure 3b shows the time evolution of the

$^{10}\text{Be}/^9\text{Be}$ ratio. The same qualitative behavior is found, such that the $^{10}\text{Be}/^9\text{Be}$ ratio peaks when $\Sigma_{\perp} \approx 0.004 \text{ g cm}^{-2}$, and very similar final $^{10}\text{Be}/^9\text{Be}$ ratios are found. Figure 4 shows the variation in final $^{10}\text{Be}/^9\text{Be}$ as a function of B_0 . For larger B_0 , the values of χ are higher and tend to exclude some GCRs, and also contraction timescales are longer, allowing more decay of ^{10}Be . For these reasons there is a tendency for $^{10}\text{Be}/^9\text{Be}$ to decrease with increasing B_0 , but the effect is small over the relevant range of B_0 . On the other hand, for smaller B_0 in the 12–15 μG range, evolution through the stage for which $\Sigma \lesssim 0.01 \text{ g cm}^{-2}$ is so rapid that trapping of ^{10}Be GCRs becomes less efficient. For even lower $B_0 < 12 \mu\text{G}$, we have fixed the evolution timescale to be 2 Myr. Thus, the $^{10}\text{Be}/^9\text{Be}$ ratio again increases with decreasing B_0 because χ is lower and there is less efficient exclusion of cosmic rays from the cloud core. Remarkably, for the range of magnetic field strengths deemed reasonable for molecular cloud cores, $10 \mu\text{G} \lesssim B_0 \lesssim 25 \mu\text{G}$ (§ 2; Crutcher 1999), the $^{10}\text{Be}/^9\text{Be}$ ratio after collapse is always in the range $(1.0\text{--}1.3) \times 10^{-3}$ (assuming $\psi = 2.0$), very consistent with the CAI ratio. Even in cloud cores that are not significantly supported against collapse by magnetic fields and that are collapsing on timescales of only $2\tau_{\text{ff}}$, there is adequate time to build up the $^{10}\text{Be}/^9\text{Be}$ ratio by trapping ^{10}Be GCRs. If our solar system formed from a molecular cloud core with initial column density $\approx 0.005 \text{ g cm}^{-2}$, comparable to the measured column densities of observed molecular cloud cores (van Dishoeck et al. 1993), then regardless of the initial magnetic field strength, the solar system would have been born with $^{10}\text{Be}/^9\text{Be} \sim 10^{-3}$. Whether the molecular cloud core was magnetically supported and evolved quiescently or had its collapse triggered by a passing supernova shock wave, we predict that all CAIs should have had the canonical meteoritic ratio $^{10}\text{Be}/^9\text{Be} \sim 10^{-3}$, due solely to contributions from GCRs.

7. CONCLUSIONS

From isotopic analyses of CAIs, the initial $^{10}\text{Be}/^9\text{Be}$ ratio of the solar system is now known to have been $\sim 10^{-3}$. Previously, significant contributions to ^{10}Be from GCRs were

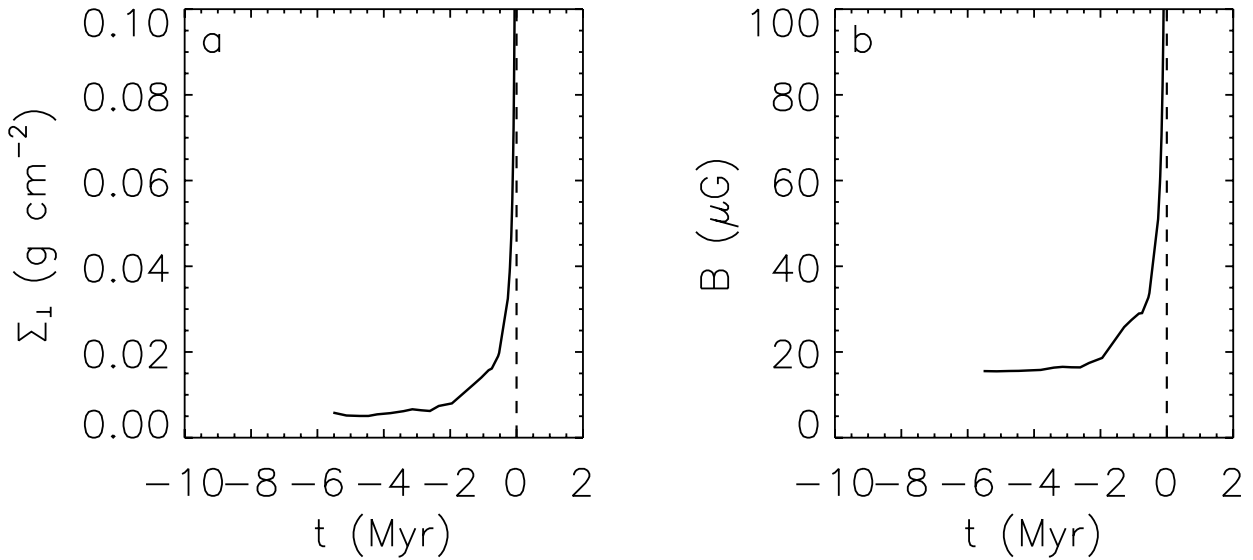


FIG. 2.—Same as Fig. 1, but extrapolated to the case $B_0 = 15 \mu\text{G}$. The cloud core now takes only half the time to form a supercritical core, but the evolution after that point is assumed to be similar to the case for $B_0 = 30 \mu\text{G}$.

ruled out (McKeegan et al. 2000b; Gounelle et al. 2001), which instead implied spallation reactions within the solar nebula, as predicted by the X-wind model (Shu et al. 2001; Gounelle et al. 2001). We have critically reexamined this conclusion by considering not just spallation reaction of GCR protons and α -particles on ambient CNO nuclei but also the trapping of GCR ^{10}Be nuclei in the molecular cloud core from which our solar system formed. We have reviewed the present-day observations of the fluxes of GCR protons, α -particles, and ^{10}Be nuclei, as well as the evidence that these fluxes were all a factor $\psi \approx 2$ higher 4.5 Gyr ago. We have numerically calculated the trapping of cosmic rays by different column densities of gas, considering magnetic mirroring and focusing and pitch angle redistribution. We calculated the time-varying rate of spallation production and trapping in the

context of the numerical simulations of cloud core collapse of DM01. We conclude that an initial ratio $^{10}\text{Be}/^9\text{Be} \sim 10^{-3}$ is a robust result, with trapping of GCR ^{10}Be nuclei accounting for $\approx 80\%$ of the initial ^{10}Be in the solar nebula.

Our conclusion that spallation reactions alone fail to explain the meteoritic $^{10}\text{Be}/^9\text{Be}$ ratio is in accord with previous results (McKeegan et al. 2000b; Gounelle et al. 2001). It is only because of *trapping* of ^{10}Be GCRs that GCR contributions can account for the meteoritic ratio. This result recalls the suggestion of Clayton & Jin (1995) that the ^{26}Al nuclei in the early solar system might have been trapped cosmic rays. They noted the coincidence between the stopping lengths of low-energy GCRs and the column densities through molecular cloud cores, $\sim 10^{-2} \text{g cm}^{-2}$. Our own estimates indicate that this fails by orders of magnitude to explain the meteoritic

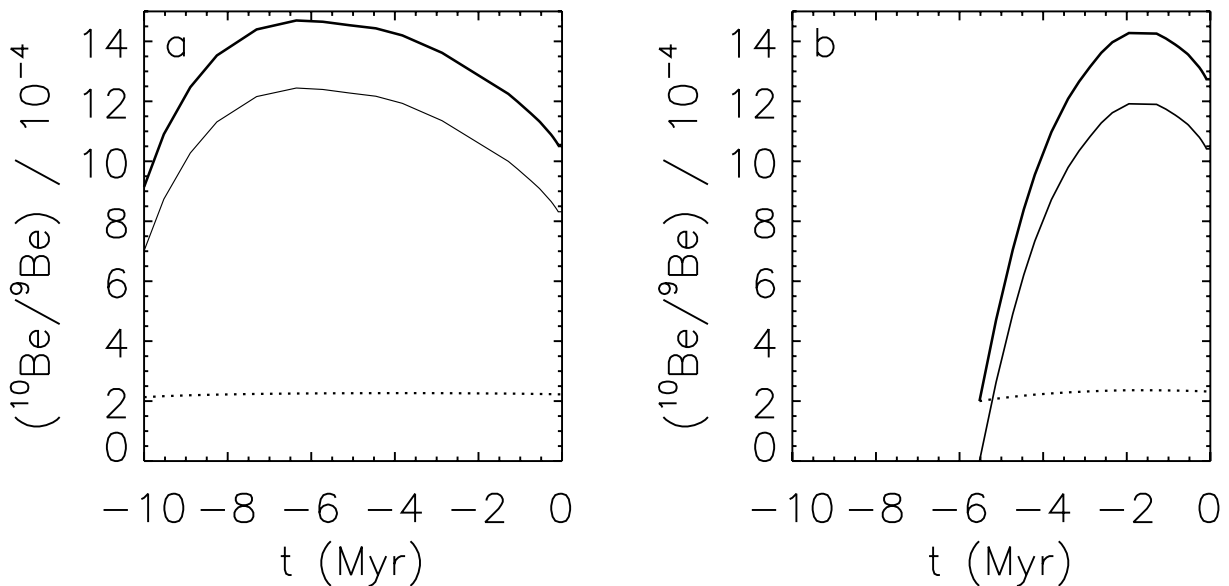


FIG. 3.—Time evolution of $^{10}\text{Be}/^9\text{Be}$ ratio in the centers of cloud cores with initial magnetic field strengths (a) $B_0 = 30 \mu\text{G}$ and (b) $B_0 = 15 \mu\text{G}$. GCR fluxes 4.5 Gyr ago a factor of $\psi = 2.0$ greater than today have been assumed. Thin dashed lines denote production rates by direct spallation reactions, thin solid lines denote rates of trapping of ^{10}Be GCRs, and thick solid lines (*top curves*) are the sum of the two contributions. Final ratios $^{10}\text{Be}/^9\text{Be} \sim 10^{-3}$ are typical.

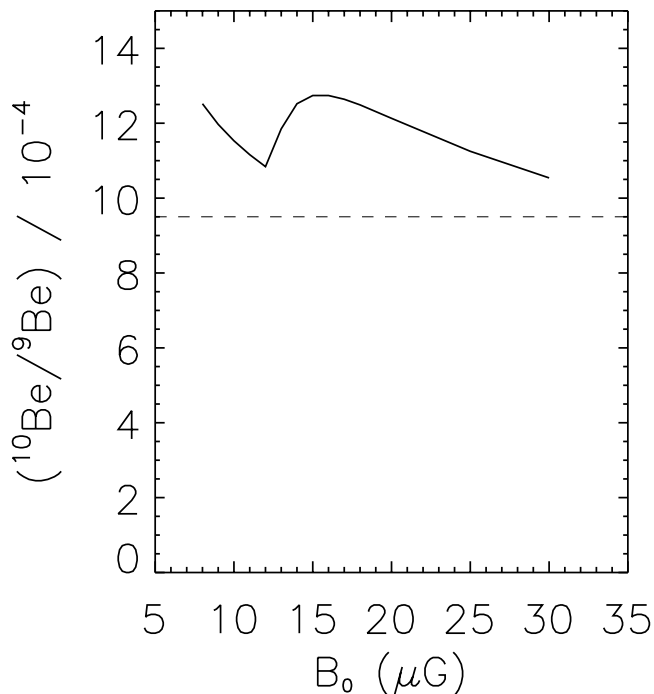


FIG. 4.—Variation of $^{10}\text{Be}/^9\text{Be}$ ratio in the centers of cloud cores as a function of their initial magnetic field strengths B_0 , assuming $\psi = 2.0$ (solid line). The $^{10}\text{Be}/^9\text{Be}$ ratio is insensitive to the initial conditions, and a value close to the meteoritic ratio 9.5×10^{-4} (dashed line) is preferred.

$^{26}\text{Al}/^{27}\text{Al}$ ratio, but the high abundance of Be nuclei in GCRs (a factor of 10^6 above solar) means that GCRs are much more likely to contribute to the beryllium abundance. We find that the mechanism of Clayton & Jin (1995) does indeed explain the initial abundance of ^{10}Be in the solar nebula.

Our firmest conclusion is that GCRs are a major contributor to the solar nebula abundance of ^{10}Be and at a minimum cannot be ruled out as a source of the ^{10}Be in CAIs. Claiming GCRs as the *sole* source of ^{10}Be carries a higher burden of proof. The uncertainties in the actual abundance are on the order of a few tens of percent; the uncertainties in the Be abundance in GCRs amount to another few tens of percent, and the uncertainties in the value of ψ also amount to several tens of percent. Altogether, we estimate an uncertainty of a factor of 3 in our results, so that GCRs might contribute as little as $\sim 30\%$ to the ^{10}Be in CAIs. Nonetheless, our best estimates of the inputs yield the result that all the ^{10}Be in CAIs can be accounted for by GCRs, and we therefore discuss the meteoritic and astrophysical implications of this result.

The first consequence is that ^{10}Be should have been spatially homogeneous in the solar nebula. A full discussion of the spatial distribution of where GCR ^{10}Be nuclei are stopped in the molecular cloud core is beyond the scope of this paper but will be considered in future work. For now, we report preliminary calculations that show that in 90% of the volume of the cloud core, the $^{10}\text{Be}/^9\text{Be}$ ratio is uniform to within 10%. Over the long timescales, ≥ 1 Myr, over which cloud cores evolve, diffusion may further homogenize the ^{10}Be , especially once the protoplanetary disk forms. The spatial homogenization of ^{10}Be in our model is to be contrasted with models of irradiation within the solar nebula, such as that of Gounelle et al. (2001), in which ^{10}Be abundance must peak near the Sun. In our model, the spatial homogeneity of ^{10}Be and the fact that ^{10}Be predates the solar nebula strongly imply that

all solid material in the solar nebula should have initially had the same canonical $^{10}\text{Be}/^9\text{Be}$ ratio. This prediction is supported by the data summarized in Table 1, from which the CAIs are seen to form with ^{10}Be ratios in the limited range $4.5 \times 10^{-4} \lesssim ^{10}\text{Be}/^9\text{Be} \lesssim 18 \times 10^{-4}$, a variation of a factor of 4 at most. In no CAI has the presence of live ^{10}Be been ruled out, including the FUN inclusion Axtell 2771.

With a canonical $^{10}\text{Be}/^9\text{Be}$ ratio established, ^{10}Be should serve as an excellent chronometer of early solar nebula events, especially since the Be-B system is more robust and less easily altered than the Al-Mg system (Sugiura et al. 2001). If the canonical ratio is 9.5×10^{-4} , then those type B CAIs with $^{10}\text{Be}/^9\text{Be} \approx 4.5 \times 10^{-4}$ must have crystallized 1.6 Myr after the first CAIs. Type B CAIs have igneous textures, petrologically constrained peak temperatures, and cooling rates consistent with melting by the chondrule-forming mechanism (see summary of Desch & Connolly 2002). This suggests that the chondrule-forming mechanism was acting 1.5 Myr after the first CAIs formed, which is consistent with the 2.7 ± 1.1 Myr interval inferred from Pb dating between CAIs (in the CV Efremovka) and chondrules (from the CR Acfer 059). Measurements capable of constraining the initial $^{10}\text{Be}/^9\text{Be}$ ratios in chondrules would confirm this interpretation. More important, measurements that conclusively show that ^{10}Be was lacking in a solid formed in the solar nebula would refute our prediction that the ^{10}Be predates the formation of the solar system.

In addition, our model explains why the presence of ^{10}Be is decoupled from that of ^{26}Al and ^{41}Ca . Whereas the ^{26}Al and ^{41}Ca once in CAIs appear to have had a common origin (Sahijpal et al. 1998), this source is known to differ from that of ^{10}Be because the FUN inclusion Axtell 2771 studied by MacPherson & Huss (2001) and the Murchison hibonites studied by Marhas et al. (2002) and Marhas & Goswami (2003) all lacked ^{26}Al and ^{41}Ca and still contained ^{10}Be . Our model demonstrates that GCRs can significantly contribute to ^{10}Be but not to any other short-lived radionuclide. Using the measured ^{26}Al GCR fluxes and the same formulation we have derived above for ^{10}Be , we calculate that the trapping of ^{26}Al GCRs yields the ratio $^{26}\text{Al}/^{27}\text{Al} \ll 10^{-8}$, orders of magnitude below the canonical ratio $^{26}\text{Al}/^{27}\text{Al} \approx 5 \times 10^{-5}$. Production of ^{26}Al by spallation of ^{27}Al or ^{26}Mg (using typical cross sections of 100 mb) yields an even smaller ratio $^{26}\text{Al}/^{27}\text{Al} \ll 10^{-9}$. Similar conclusions were reached by Ramaty et al. (1996), who showed that if ^{26}Al were produced by spallation then Be would be overproduced. We likewise find that GCR contributions to ^{41}Ca are negligible. Thus, GCR contributions can contribute to ^{10}Be but not to these other short-lived radionuclides, which must share a common but separate source. This source is almost certainly a supernova explosion, on the basis of the new evidence that the solar nebula contained live ^{60}Fe (Tachibana & Huss 2003; Mostefaoui et al. 2003). This isotope is particularly difficult to explain by spal-lative processes (Lee et al. 1998).

The experimentally confirmed decoupling of ^{10}Be from the other radionuclides is consistent with the scenario we have outlined above, in which GCRs contribute to ^{10}Be alone but a supernova contributes to all the other short-lived radionuclides. It is *not* consistent with models in which spallation within the solar nebula produces all the radionuclides. In situ irradiation models also have the difficulty that ^{10}Be would almost certainly be overproduced. For example, in the X-wind model of Gounelle et al. (2001), where C and N and most of the O atoms are neglected, and the energetic particle flux has a significant ^3He component (to enhance production of ^{26}Al),

^{10}Be is nearly overproduced relative to ^{26}Al . Moreover, the chemistry of CAI minerals constrains the formation of CAIs to take place in a reducing solar-composition gas (see review by Krot et al. 2000), not the X-wind environment in which CAI formation takes place in a gas 10^7 times more oxidizing than a solar-composition gas (Shu et al. 2001). Restoring a solar-composition gas (with its CNO nuclei) only increases the number of nuclei that can be spalled to create ^{10}Be (by about an order of magnitude), exacerbating the problem of overproduction of ^{10}Be . We conclude that in situ irradiation models generally overproduce ^{10}Be and cannot in any case explain the decoupling of ^{10}Be and the other radionuclides.

It is hoped that future research will better constrain the inputs to our calculations and sharpen these conclusions. More precisely measured $^{10}\text{Be}/^9\text{Be}$ ratios, in a greater number of objects, will tighten the constraints on the canonical $^{10}\text{Be}/^9\text{Be}$ ratio. The elucidation of how magnetohydrodynamic turbulence would affect the propagation of cosmic rays through molecular cloud cores would test the validity of our assumption that turbulence is unimportant. Continued spacecraft measurements of GCR fluxes will reduce the uncertainties in the low-energy ^{10}Be flux. More detailed models of Galactic chemical evolution and Li, Be, and B production may yield better convergence on the enhancement of GCR flux 4.5 Gyr ago (ψ). Alternatively, models of the chemistry of the early solar system may better constrain ψ directly. Aikawa et al. (1999) have considered the effect that variations in the GCR ionization rate in the comet-forming region would have had on chemical abundances in comets. Their Figure 7 shows a particular sensitivity of the HCN/CH_4 ratio on the cosmic-ray ionization rate. Our presumed value of $\psi \approx 2$, multiplying the cosmic-ray ionization rate of the interstellar GCR flux, $\zeta \approx (3-4) \times 10^{-17} \text{ s}^{-1}$ (Webber 1998), yields $\zeta \approx 7 \times 10^{-17} \text{ s}^{-1}$

and the ratio $\text{HCN}/\text{CH}_4 \approx 0.2$ (interpolating between the cases $\zeta \approx 1.3 \times 10^{-17}$ and $1.3 \times 10^{-16} \text{ s}^{-1}$). This matches exactly the ratio $\text{HCN}/\text{CH}_4 \approx 0.2$ observed for comet Hale-Bopp (see Table 3 of Aikawa et al. 1999). Continued modeling and cometary observations may be the best way to constrain the GCR flux in the early solar system.

Continued work should sharpen the debate, yet we are confident in saying that a large fraction of the ^{10}Be once in CAIs is attributable to GCRs, through a combination of trapping of ^{10}Be nuclei and GCR-induced spallation reactions. Since such contributions are not ruled out, the one-time presence of ^{10}Be in CAIs is not a “smoking gun” for in situ irradiation models such as the X-wind model (Gounelle et al. 2001). Indeed, because such models tend to overproduce ^{10}Be and cannot explain the decoupling of ^{10}Be from the other radionuclides and because GCR contributions can plausibly explain all the initial ^{10}Be abundance, we argue that ^{10}Be and ^{10}Be alone has a cosmic-ray origin, while the other short-lived radionuclides share a common but separate origin. A cosmic-ray origin for ^{10}Be makes the testable prediction that all solids formed in the early solar system should have had $^{10}\text{Be}/^9\text{Be}$ ratios near the canonical value, with variations attributable to different times of crystallization, making the Be-B system an excellent chronometer. The newly discovered evidence for live ^{60}Fe at the birth of the solar system suggests a supernova origin for the other short-lived radionuclides.

We are pleased to thank Shantanu Basu, Marc Chaussidon, Donald Clayton, Kuljeet Marhas, Kevin McKeegan, and Francois Robert for helpful discussions, and Pat Cassen, Eugene Chiang, Larry Nittler, and an anonymous reviewer for critical readings of an earlier version of the manuscript.

REFERENCES

- Aikawa, Y., Umebayashi, T., Nakano, T., & Miyama, S. M. 1999, *ApJ*, 519, 705
- Allende Prieto, C., Lambert, D. L., & Asplund, M. 2001, *ApJ*, 556, L63
- Anders, E., & Grevesse, N. 1989, *Geochim. Cosmochim. Acta*, 53, 197
- Barry, D. C. 1988, *ApJ*, 334, 436
- Basu, S. 2000, *ApJ*, 540, L103
- Bethe, H. A. 1933, in *Handbuch der Physik*, Vol. 24, Part 1, ed. H. Geiger & K. Scheel (2d ed.; Berlin: Springer), 491
- Bourke, T. L., Myers, P. C., Robinson, G., & Hyland, A. R. 2001, *ApJ*, 554, 916
- Cameron, A. G. W. 2001, *ApJ*, 562, 456
- Cameron, A. G. W., & Truran, J. W. 1977, *Icarus*, 30, 447
- Caselli, P., Walmsley, C. M., Terzieva, R., & Herbst, E. 1998, *ApJ*, 499, 234
- Chandran, B. D. G. 2000, *ApJ*, 529, 513
- Chandrasekhar, S., & Fermi, E. 1953, *ApJ*, 118, 113
- Chang, R., Shu, C. S., & Hou, J. 2002, *Chinese J. Astron. Astrophys.*, 2, 226
- Chaussidon, M., Robert, F., McKeegan, K. D., & Krot, A. N. 2001, *Lunar Planet. Inst. Conf.*, 32, 1862
- Ciolek, G. E., & Basu, S. 2001, *ApJ*, 547, 272
- Ciolek, G. E., & Mouschovias, T. Ch. 1995, *ApJ*, 454, 194
- Clayton, D. D., & Jin, L. 1995, *ApJ*, 451, 681
- Crutcher, R. M. 1999, *ApJ*, 520, 706
- Desch, S. J., & Connolly, H. C. 2002, *Meteoritics Planet. Sci.*, 37, 183
- Desch, S. J., & Mouschovias, T. Ch. 2001, *ApJ*, 550, 314 (DM01)
- Duvernois, M. A., & Thayer, M. R. 1996, *ApJ*, 465, 982
- Dwek, E. 1998, *ApJ*, 501, 643
- Ellison, D. C., Drury, L. O., & Meyer, J. 1997, *ApJ*, 487, 197
- Engelmann, J. J., Ferrando, P., Soutoul, A., Goret, P., & Juliusson, E. 1990, *A&A*, 233, 96
- Ferrando, P., Lal, N., McDonald, F. B., & Webber, W. R. 1991, *A&A*, 247, 163
- . 1993, *ApJ*, 415, 680
- Firestone, R. B., Shirley, V. S., Baglin, C. M., Chu, S. Y. F., & Zipkin, J. 1996, *Table of Isotopes* (New York: Wiley)
- Goswami, J. N., Marhas, K. K., & Sahijpal, S. 2001, *ApJ*, 549, 1151
- Goswami, J. N., & Vanhala, H. A. T. 2000, in *Protostars and Planets IV*, ed. V. Mannings, A. P. Boss, & S. S. Russell (Tucson: Univ. Arizona Press), 963
- Gounelle, M., Shu, F. H., Shang, H., Glassgold, A. E., Rehm, K. E., & Lee, T. 2001, *ApJ*, 548, 1051
- Hunter, S. D., et al. 1997, *ApJ*, 481, 205
- Ip, W.-H., & Axford, W. I. 1985, *A&A*, 149, 7
- Krot, A. N., Fegley, B., Lodders, K., & Palme, H. 2000, *Protostars and Planets IV*, ed. V. Mannings, A. P. Boss, & S. S. Russell (Tucson: Univ. Arizona Press), 1019
- Kulsrud, R., & Pearce, W. P. 1969, *ApJ*, 156, 445
- Lee, T., Shu, F. H., Shang, H., Glassgold, A. E., & Rehm, K. E. 1998, *ApJ*, 506, 898
- Lemoine, M., Vangioni-Flam, E., & Casse, M. 1998, *ApJ*, 499, 735
- Lerche, I., & Schlickeiser, R. 1982, *MNRAS*, 201, 1041
- Lukasiak, A., Ferrando, P., McDonald, F. B., & Webber, W. R. 1994, *ApJ*, 426, 366
- MacPherson, G. J., & Huss, G. R. 2001, *Lunar Planet. Inst. Conf.*, 32, 1882
- Marhas, K. K., & Goswami, J. N. 2003, *Lunar Planet. Inst. Conf.*, 34, 1303
- Marhas, K. K., Goswami, J. N., & Davis, A. M. 2002, *Science*, 298, 2182
- Marsakov, V. A., Shevelev, I. G., & Suchkov, A. A. 1990, *Ap&SS*, 172, 51
- McKeegan, K. D., Chaussidon, M., & Robert, F. 2000a, *Lunar Planet. Inst. Conf.*, 31, 1999
- . 2000b, *Science*, 289, 1334
- Meusinger, H. 1991, *Ap&SS*, 182, 19
- Meyer, J., Drury, L. O., & Ellison, D. C. 1997, *ApJ*, 487, 182
- Mori, M. 1997, *ApJ*, 478, 225
- Morrissey, D. J. 1989, *Phys. Rev. C*, 39, 460
- Mostefaoui, S., Lugmair, G. W., Hoppe, P., & El Goresy, A. 2003, *Lunar Planet. Inst. Conf.*, 34, 1585
- Mouschovias, T. Ch. 1991, *ApJ*, 373, 169
- Mouschovias, T. Ch., & Spitzer, L. 1976, *ApJ*, 210, 326
- Nath, B. B., & Biermann, P. L. 1994, *MNRAS*, 267, 447
- Ossenkopf, V., & Mac Low, M.-M. 2002, *A&A*, 390, 307
- Prantzos, N., Casse, M., & Vangioni-Flam, E. 1993a, *ApJ*, 403, 630
- Prantzos, N., Vangioni-Flam, E., & Casse, M. 1993b, in *Origin and Evolution of the Elements*, ed. N. Prantzos, E. Vangioni-Flam, & M. Casse (Cambridge: Cambridge Univ. Press)

- Ramaty, R., Kozlovsky, B., & Lingenfelter, R. E. 1996, *ApJ*, 456, 525
- Read, S. M., & Viola, V. E. 1984, *At. Data Nucl. Data Tables*, 31, 359
- Rocha-Pinto, H. J., Scalo, J., Maciel, W. J., & Flynn, C. 2000, *A&A*, 358, 869
- Sahijpal, S., Goswami, J. N., Davis, A. M., Lewis, R. S., & Grossman, L. 1998, *Nature*, 391, 559
- Scalo, J. M., Barry, D. C., & Sneden, C. 1987, *BAAS*, 19, 1108
- Shu, F. H., Allen, A., Shang, H., Ostriker, E. C., & Li, Z. 1999, in *The Origin of Stars and Planetary Systems*, ed. C. J. Lada & N. Kylafis (NATO ASI Ser. C, 540; Dordrecht: Kluwer), 193
- Shu, F. H., Shang, H., Glassgold, A. E., & Lee, T. 1997, *Science*, 277, 1475
- Shu, F. H., Shang, H., Gounelle, M., Glassgold, A. E., & Lee, T. 2001, *ApJ*, 548, 1029
- Shu, F. H., Shang, H., & Lee, T. 1996, *Science*, 271, 1545
- Srinivasan, G. 2002, *Meteoritics Planet. Sci. Suppl.*, 37, A135
- Stone, J. M., & Norman, M. L. 1992a, *ApJS*, 80, 753
- . 1992b, *ApJS*, 80, 791
- Sugiura, N., Shuzou, Y., & Ulyanov, A. 2001, *Meteoritics Planet. Sci.*, 36, 1397
- Tachibana, S., & Huss, G. R. 2003, *ApJ*, 588, L41
- Tamura, M., Hough, J. H., & Hayashi, S. S. 1995, *ApJ*, 448, 346
- Tomisaka, K., Ikeuchi, S., & Nakamura, T. 1988, *ApJ*, 335, 239
- Twarog, B. A. 1980, *ApJ*, 242, 242
- Umebayashi, T., & Nakano, T. 1981, *PASJ*, 33, 617
- Valle, G., Ferrini, F., Galli, D., & Shore, S. N. 2002, *ApJ*, 566, 252
- van der Tak, F. F. S., & van Dishoeck, E. F. 2000, *A&A*, 358, L79
- van Dishoeck, E. F., Blake, G. A., Draine, B. T., & Lunine, J. I. 1993, in *Protostars and Planets III*, ed. E. Levy & J. Lunine (Tucson: Univ. Arizona Press), 163
- Vangioni-Flam, E., Audouze, J., Oberto, Y., & Casse, M. 1990, *ApJ*, 364, 568
- Ward-Thompson, D. 2002, *Science*, 295, 76
- Webber, W. R. 1998, *ApJ*, 506, 329
- Webber, W. R., Lukasiak, A., & McDonald, F. B. 2002, *ApJ*, 568, 210
- Wielen, R., Fuchs, B., & Dettbarn, C. 1996, *A&A*, 314, 438
- Williams, J. P., Bergin, E. A., Caselli, P., Myers, P. C., & Plume, R. 1998, *ApJ*, 503, 689
- Yanasak, N. E., et al. 2001, *ApJ*, 563, 768
- Zweibel, E. G., & Heiles, C. 1997, *Nature*, 385, 131